ISSN 0256-4637

VOLUME 39 NUMBER 4 OCTOBER-DECEMBER 2017

Journal of Pure and Applied

Ultrasonics

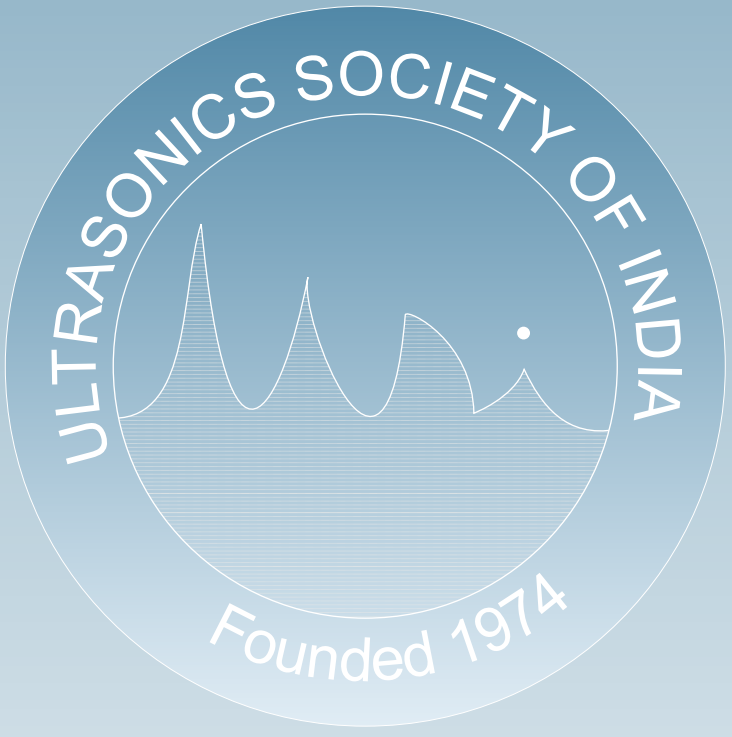

Website : www.ultrasonicsindia.org

A Publication of Ultrasonics Society of India

A Quarterly Publication of Ultrasonics Society of India

Journal of Pure and Applied

Ultrasonics

No. 4	Volume 39	October-December 2017

SUBSCRIPTION (postage paid)

Single	Rs. 750/-	US$ 60/-
Annual	Rs. 3000/-	US$ 250/-
USI *members*	Free	

ADVERTISEMENT

The Journal offers opportunity of wide and effective publicity for the manufacturer, suppliers of ultrasonic equipment, devices and materials and also for scientific instruments and components. Tariff is as follows :

Back Cover	Rs. 5000/-	US $ 200/-
Inside Cover	Rs. 3000/-	US $ 150/-
Full page	Rs. 2000/-	US $ 100/-
Half page	Rs. 1500/-	US $ 60/-

Discount of 20% is admissible for 4 successive insertions.

The submission of papers and all other correspondence regarding the Journal may please be addressed to :

Publication Secretary
Journal of Pure and Applied Ultrasonics
C/o Ultrasonics Society of India
CSIR-National Physical Laboratory
Dr. K.S. Krishnan Road, New Delhi-110012
publicationsecretary.usi@gmail.com
www.ultrasonicsindia.org

ISSN 0256–4637

Journal of Pure and Applied Ultrasonics

VOLUME 39 NUMBER 4 OCTOBER–DECEMBER 2017

CONTENTS

(Authors have stated that the papers have not been published elsewhere)

Website : www.ultrasonicsindia.org

A Publication of — Ultrasonics Society of India

J. Pure Appl. Ultrason. 39 (2017) pp. 103-109

Temperature dependent ultrasonic characterization of wurtzite boron nitride

Chandreshvar Prasad Yadav* and Dharmendra Kumar Pandey

Department of Physics, P.P.N. (P.G.) College,
Kanpur-208 001, India
*E-mail: cpy99physics@gmail.com

The present study encloses the evaluation of second order elastic constants of wurtzite boron nitride (w-BN) in temperature range 300K-1800K using the many body interaction potential model approach. Orientation and temperature dependent ultrasonic velocity, thermal relaxation time and other related thermo-physical parameters (Debye average velocity, Debye temperature,specific heat, thermal energy density and thermal conductivity) are also calculated using evaluated second order elastic constants and other known parameters of w-BN. It is found that thermal relaxation time is least for the wave propagation along 55° from the unique axis of crystal at each temperature. The orientation dependent thermal relaxation time of w-BN is predominantly affected by the Debye average velocity while the temperature dependent thermal relaxation time is governed by thermal conductivity. The calculated elastic and ultrasonic properties of w-BN are compared with the properties of other wurtzite structured materials for the complete analysis and characterization of material.

Keywords: Elastic constants, ultrasonic velocities, thermal conductivity, thermal relaxation time.

Introduction

Boron nitride is low porosity white solid material. Boron nitride (BN) can stably exist in many polymorphs because B and N atoms can bind together by sp^2 and sp^3 hybridizations. Boron nitride can be found in hexagonal/ layered graphite like phase (h-BN, r-BN), turbostratic (t-BN), cubic diamond-like phase (c-BN), wurtzite-like phase (w-BN), layered graphite-like phase (h-BN or r-BN)[1,2]. The boron nitride is normally found in the hexagonal phase. Hexagonal boron nitride (h-BN) is the stable phase under ambient conditions while cubic BN and wurtzite BN were synthesized from h-BN at high temperature and high pressure[1-3].

The wurtzite phase of BN phase is metastable phase in nature. The keen interest for the study of this material is due to its technological features like extreme hardness, high melting point, interesting dielectric and thermal behaviour. Structural, mechanical, electronic properties, and stability of boron nitride (BN) in *Pnma* structure were studied using first-principles calculations by Cambridge Serial Total Energy Package (CASTEP) plane-wave code, and the calculations were performed with the local density approximation[4]. Thermal conductivity of h-BN, c-BN, t-BN, r-BN and its composites are reported elsewhere[1,2,5,6]. For the thermal management applications, BN is found to be electrically insulating counterpart of graphene[7,8]. Insulating behaviour of this material along with its high thermal conductivity generates a new concept for the electronic industry.

The structural, elastic, mechanical and acoustical properties of different phases of BN were determined by several researcher using X-ray diffraction, pseudo-potential, DFT methods[1,2,9-14]. Wurtzite phase of BN belong to III group nitrides as GaN, AlN, InN[13,14] but very few work have been performed for the elastic, thermal and ultrasonic characterization of w-BN. Therefore the present study is focused on the elastic and ultrasonic characterization of w-BN.

The theoretical evaluation of second order elastic constants of wurtzite boron nitride (w-BN) has been performed in temperature range 300K-1800K using the many body interaction potential model approach. Orientation/temperature dependent ultrasonic velocity, thermal relaxation time and other related thermo-physical parameters (Debye average velocity, Debye temperature,

specific heat, thermal energy density, density and thermal conductivity) are also calculated using evaluated second order elastic constants and density values. The obtained results of w-BN are compared with the properties of other wurtzite structured materials for the complete analysis and characterization.

Theory

Elastic constants

The hexagonal structured crystals are mainly classified to close packed (hcp) and wurtzite (wz) structures. It has long been recognized that the crystals having wurtzite (wz) and sphalerite (zinc blende or ZB) structures are fundamentally similar despite differences between the two structures[15]. ZB crystals are fcc with two atoms per primitive cell, where as wz crystals are hexagonal (C_{6V}) with four atoms per cell. The fundamental relation between the two structures is that the local environment of any atom in either ZB or ideal wz (c/a=1.633) is exactly the same through the second neighbour[15]. The hexagonal structured crystals have maximum packing fraction similar to fcc. The fraction of the total volume occupied by the atoms is 0.74 for both structures[16]. The formulation for calculating the second order elastic constants of hexagonal structured crystals are performed using many body interaction up to second nearest neighbour between the atoms. The expressions for the elastic constants are given in our previous paper[17].

The bulk modulus (B) of wurtzite structure material can be determined by following expression using the second order elastic constants.

$$B_0 = \frac{(C_{11}+C_{12})C_{33}-2C_{13}^2}{C_{11}+C_{12}+2C_{33}-4C_{13}} \quad (1)$$

Ultrasonic velocity

There are three types of acoustical wave velocity in hexagonal structured crystals as one longitudinal and two shear wave velocities that are well related to the second order elastic constants. The velocities can be found in literature[18].

The density of wurtzite structured material can be determined by following expression[19].

$$\rho = \frac{2\,M\,n}{3\sqrt{3}\,a^2 c N_A} \quad (2)$$

Where M, N_A and n are molecular weight, Avogadro number and number of atoms per unit cell respectively.

Debye average velocity is an important parameter in the low temperature physics because it is related to elastic constants through ultrasonic velocities. The expression for Debye average velocity (V_D) is given in literature[18].

On the knowledge of elastic constants, the theoretical evaluation of ultrasonic velocity can be done. Debye temperature (T_D) is indirectly related to elastic constants through Debye average velocity[18].

The time taken for re-establishment of equilibrium of the thermal phonons is called the thermal relaxation time (τ) and is given by the following equation:

$$\tau = 3\,k / C_V\ V_D^2 \quad (3)$$

Here τ is thermal relaxation time. The quantities k and C_V are the thermal conductivity and specific heat per unit volume of the material. The specific heat per unit volume is function of T_D/T and can be determined from literature[20,21]. The thermal conductivity of wurtzite structured material can be determined by following expression[22].

$$k = \frac{AMT_D{}^3\delta^3}{\gamma^2 T n^{2/3}} \quad (4)$$

Where, A is a constant; M is the molecular weight; δ^3 is volume per atom; γ is Grüneisen number; T is the temperature. The constant A is depends on the Grüneisen number and is given by following expression.

$$A = \frac{2.43\times10^{-8}}{1-0.514/\gamma+0.228/\gamma^2} \quad (5)$$

Results and Discussion

For the evaluation of temperature dependent second order elastic constants of w-BN, the lattice parameters (a and c) are taken from the literature[1,13]. The value of m and n for wurtzite boron nitride are taken 6 and 7 respectively. Lennard Jones constant b_0 for w-BN is determined under equilibrium condition and is 7.44×10^{-65} erg-cm^7. The temperature dependent second order elastic constants are calculated using temperature dependent lattice parameters, *m, n and* b_0. Temperature dependent bulk modulus are evaluated with help of Eq.(1) and calculated second order elastic constants. The obtained SOECs and bulk modulus are given in Table 1.

Table 1 – Parameters of w-BN at different temperature and at zero pressure.

Temperature→ Parameter ↓	300K	500K	700K	900K	1100K	1300K	1500K	1700K	1800K
a (Å)	2.550	2.551	2.553	2.555	2.558	2.560	2.563	2.566	2.568
c (Å)	4.200	4.203	4.206	4.209	4.214	4.218	4.223	4.228	4.230
ρ (10^3 kg/m^3)	3.512	3.506	3.499	3.490	3.480	3.469	3.456	3.444	3.438
C_{11} (GPa)	816.1	812.9	806.6	800.3	790.9	784.8	775.6	766.6	760.7
C_{12} (GPa)	200.4	199.6	198.1	196.5	194.2	192.7	190.5	188.3	186.8
C_{13} (GPa)	176.8	176.1	174.8	173.4	171.4	170.0	168.1	166.1	164.8
C_{33} (GPa)	863.1	859.7	853.1	846.4	836.5	830.0	820.3	810.8	804.5
C_{44} (GPa)	212.1	211.2	209.6	207.9	205.6	203.9	201.6	199.2	197.7
C_{66} (GPa)	320.0	318.8	316.3	313.8	310.2	307.8	304.2	300.6	298.3
B (GPa)	400.3	398.8	395.6	392.6	387.9	384.9	380.5	376.1	373.1
T_D (K)	1436.5	1434.1	1428.9	1424.0	1416.4	1411.6	1404.2	1396.8	1391.8

The density is function of lattice parameters[19]. The obtained density values are presented in Table 1. The ultrasonic velocities are evaluated with help of SOECs and densities for ultrasonic wave propagation at different orientation from the unique axis of w- BN crystal. The Debye average velocity at different temperature and orientation from unique axis are calculated. The ultrasonic velocities V_1, V_2, V_3 and V_D are shown in Figs. 1-4. The Debye temperature of w-BN is calculated at different temperature which is shown in Table 1. The specific heat at constant volume

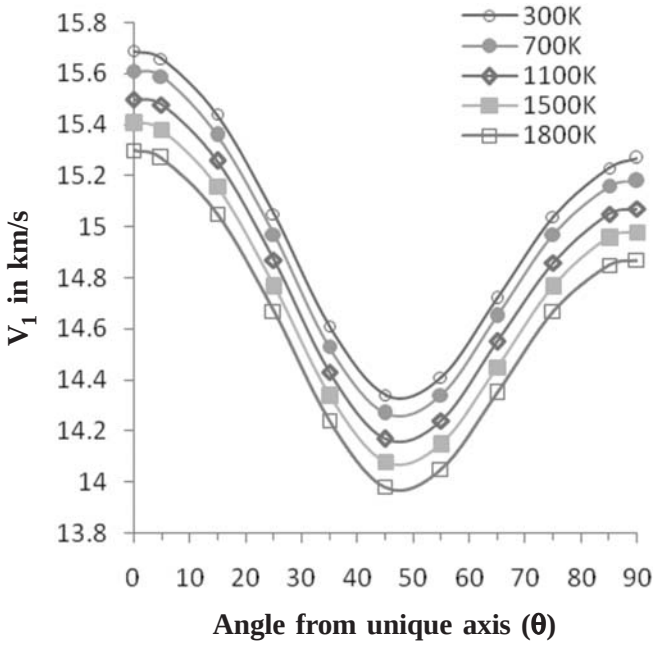

Fig. 1 Longitudinal wave velocity vs angle from unique axis of w-BN crystals

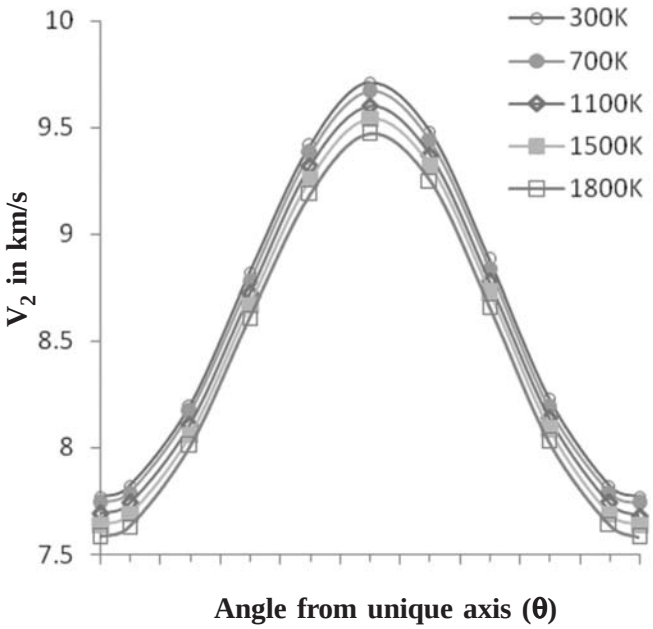

Fig. 2 Quasi shear wave velocity vs angle from unique axis of w-BN crystal

(C_V) and energy density *(E_0)* is obtained using Debye temperature and literature[21]. The values of C_V and E_O are shown Fig. 5. TheGruneisen number for BN is 0.7[22] and the δ can be determined with formula given elsewhere[19]. The thermal relaxation time and thermal conductivity are determined with the help of Eqs. (3)-(4) using C_V, and V_D at different temperature for wave propagation along unique axis of the w-BN crystal. Orientation and temperature dependent k and τ are plotted in Figs. 6-7.

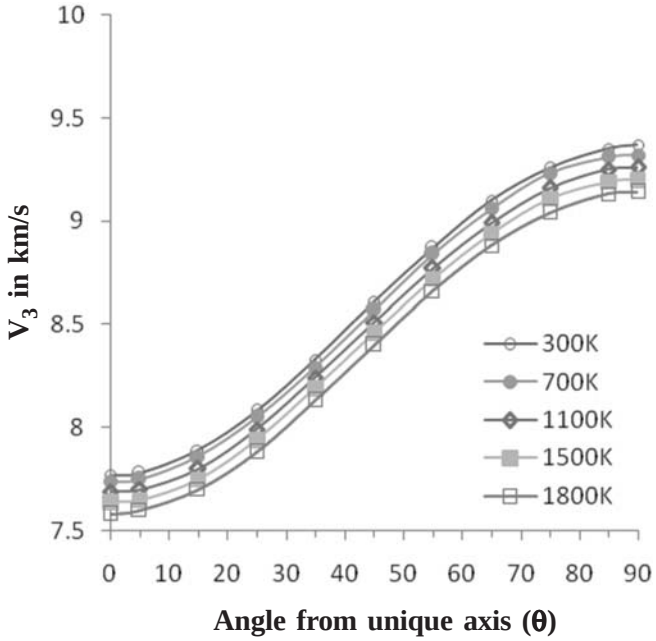

Fig. 3 Shear wave velocity vsangle from unique axis of w-BN crystal

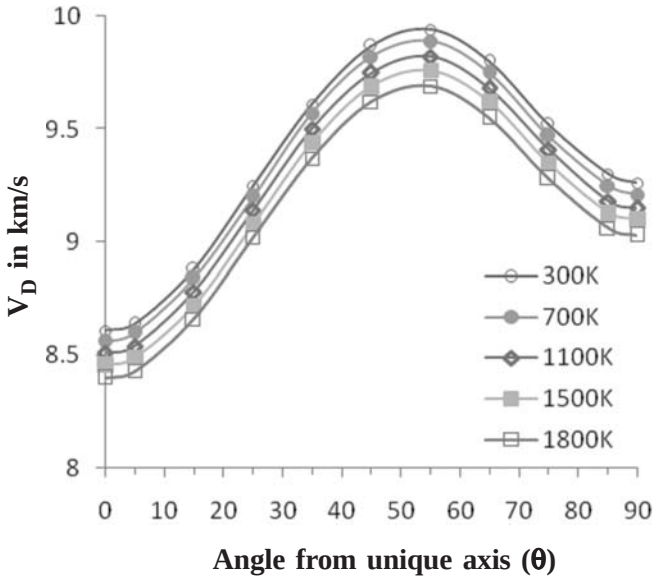

Fig. 4 Debye average velocity vs angle from unique axis of w-BN crystal

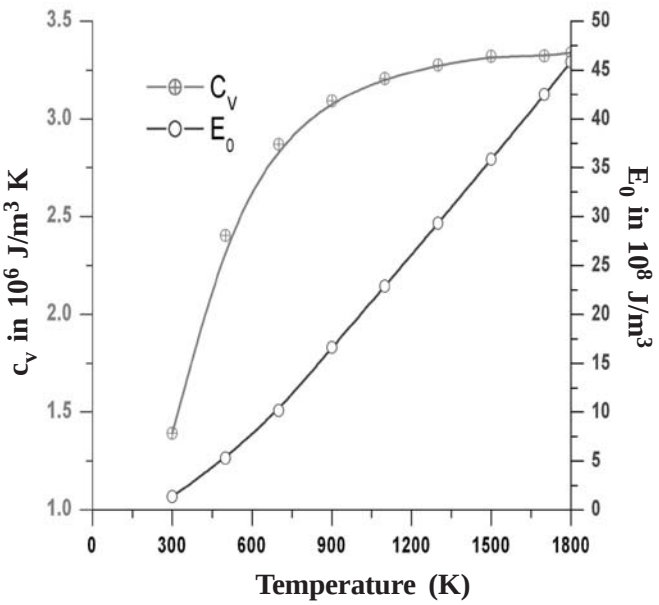

Fig. 5 C_V and E_0 vs temperature for w-BN crystal

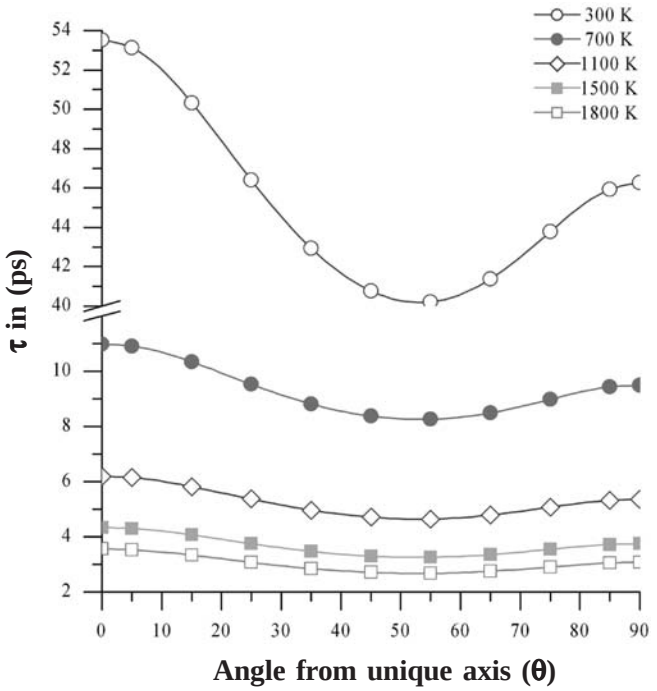

Fig. 6 Thermal relaxation time (τ) vs angle from unique axis for w- BN crystal

A perusal of Table 1 indicates that all calculated second order elastic constants and bulk modulus decrease with the temperature. Since the lattice parameter of w-BN crystal increases with temperature[13] therefore inter-atomic distance increases and hence the inter-atomic force reduces with the temperature. This causes reduction in stress bearing capacity of material. Therefore decrease in elastic constant values with temperature is obtained.

The SOEC C_{11}, C_{33} and bulk modulus B_0 of w-BN has been reported 982GPa, 1077GPa and 400GPa respectively at 300K elsewhere[1,23]. The present bulk modulus at 300K is exactly same with reported value. The values C_{11} and C_{33} at 300K are also very close to their corresponding reported values and a slight

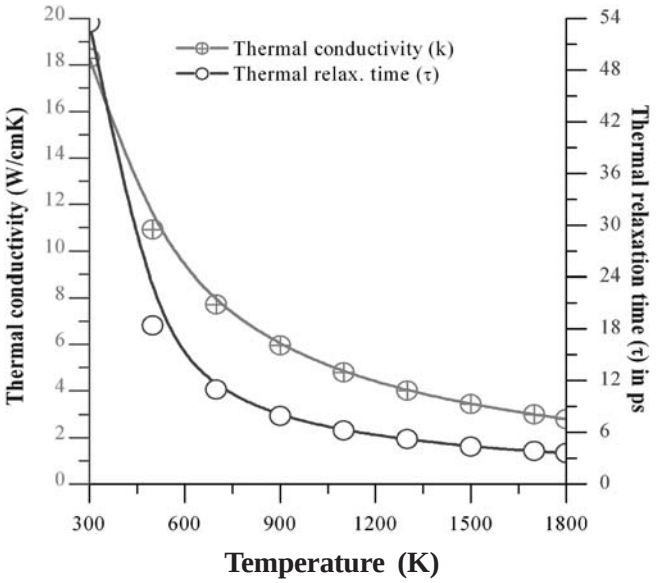

Fig. 7 Thermal conductivity and thermal relaxation time vs temperature for w-BN crystal

difference is due to the reason that the interaction in present model is considered up to second nearest neighbuors. Thus present SOECs of w-BN at different temperature under potential model approach is justified. Since our potential model approach for evaluation of second order elastic constants needs only lattice parameter at initial and provides good results and avoids approximations as required in first principle calculations therefore it is better than the other model. The density of hexagonal wurtzite structured material is inversely proportional to a^2c and the lattice parameters of selected material is reported to increase with temperature[13] hence the calculated density of w-BN at different temperature is found to decrease with temperature (Table 1). The elastic constants of w-BN are found too large in comparison to same group nitrides (AlN, GaN, InN)[24]. Therefore the mechanical behaviour will be better than the same group nitrides. The mechanical strength, hardness and durability of the material are related to their anisotropic elastic constants, so the SOECs of w-BN are important in the field of material preparing industries.

The present value of density of w-BN at 300K is 3.512 g/cc and the density given in literature[1] is 3.487 g/cc. Therefore our method for calculation of temperature dependent density is justified. On the basis of mode of propagation there are four types of ultrasonic velocities, as longitudinal, shear, surface and lamb wave velocity. Longitudinal and shear wave velocities are more important for the material characterization because they are well related to elastic constants and density. The elastic constants of material are related with the fundamental solid state phenomenon such as specific heat, Debye temperature and Grüneisen parameters. Elastic constants are related to inter-atomic forces, coordination changes *etc.*, and also with the fracture, porosity, crystal growth and microstructural factors (grain shape, grain boundaries, texture and precipitates *etc.*). Thus, the mechanical behaviour and anisotropic properties of the material under different physical condition (temperature, pressure, concentration, composition, size *etc.*) can be well defined on the knowledge of ultrasonic velocity.

The temperature dependent ultrasonic velocities (V_1, V_2, V_3) and Debye average velocity (V_D) of w-BN crystal at different orientation (Figs.1-3) reveal that all the ultrasonic velocities decrease with temperature while their nature with orientation resembles the same characteristics as the same group of nitrides[24]. The longitudinal ultrasonic velocity (V_1) is minimum along $\theta = 45°$ for w-BN material and quasi shear wave velocity (V_2) is maximum along $\theta = 45°$ while pure shear wave velocity (V_3) increases with the direction of orientation with unique axis. The ultrasonic velocity is directly proportional to square root of elastic constant and inversely proportional to square root of density. Yet, both the second order elastic constants and density of w-BN are found to decrease with temperature but the elastic constants play dominating role towards the reduction in ultrasonic velocity with temperature. As the elastic constants of w-BN are found very high in comparison to elastic constants of the same group of nitrides (AlN, GaN, InN) therefore the ultrasonic velocities of w-BN have largest value among IIIrd group nitrides. The present value of V_1 and V_2 or V_3 for wave propagation along <001> direction ($\theta = 0°$) at 300K are 15.7 km/s and 7.8 km/s respectively, while the same velocity[23] values for same direction of propagation are reported to be 17.6 km/s and 10.5 km/s. The good resemblance between reported and present value of velocities authenticate our evaluated data of ultrasonic velocities.

For the determination of specific heat of material, the essential parameter is Debye temperature which is directly co-related with Debye average velocity[20]. The Debye temperature of w-BN is found to decrease with temperature (Table 1), as the Debye temperature is indirectly related to elastic constants through Debye

average velocity. The reported Debye temperature[1,13] at 300 K in literature is 1400 K while the present value is 1436.5 K. The first principle calculation reports that the Debye temperature of w-BN decreases with temperature[25]. The similarity between present and reported Debye temperature reveals its justification.

Figure 5 indicates that specific heat and thermal energy density of w-BN increases with temperature. The similar characteristic[25] of w-BN has been reported for C_V. The present value of C_V at zero pressure and 300K is 1.39 J/cm^{3}K (11.65 J/mole K), while the reported value of C_V at same condition in literature is 11.124 J/mole K. The atoms of crystal go away due to increase in lattice parameter. Therefore the loss of heat energy by the collision of surrounding atoms decreases. Therefore C_V of w-BN is found to increases with temperature.

It is obvious from Figs. 6-7 that the thermal conductivity and thermal relaxation time of w-BN decreases with temperature. It can also be seen from Fig. 6 that thermal relaxation time of w-BN decreases with orientation up to $\theta = 55°$ and then increases. The thermal relaxation time is well co-related with thermal conductivity, Debye average velocity and specific heat of material [Eq. (3)]. Thermal conduction is a property of material that measures easiness of heat energy transfer through acoustic vibrations. The bond length/lattice parameter of material increases with temperature. This causes reduction in Brillouin zone and hence Debye frequency and Debye temperature reduce. Due to reduction in Debye frequency, the heat transfer through acoustic vibrations reduces. Therefore thermal conductivity of w-BN is found to decay with temperature.

From Fig. 7, it is clear that temperature dependent thermal relaxation time of w-BN is predominantly affected by thermal conductivity and decreases with temperature. When the ultrasonic wave propagates through crystalline media then there is interaction of phonons of ultrasonic wave and crystal lattice vibrations. Due to this, thermal energy distribution of thermal phonons is disturbed. The re-establishment time of thermal phonons is termed as thermal relaxation time. The transfer of momentum among atoms through acoustic vibrations becomes slow as temperature increases due to increase in atomic separation. This results least disturbance in thermal energy distribution of thermal phonons. Therefore the re-establishment time for thermal phonons reduces with temperature. Phonon-phonon interaction is one of the major cause for the ultrasonic attenuation in pure crystalline medium[18]. Therefore it can be predicted that ultrasonic attenuation due to phonon-phonon interaction in w-BN will decrease with temperature. τ for w- BN is of pico-second order which is of same order as reported for similar nitride groups in literature[24]. The thermal relaxation time of w-BN is received 53.5 ps at 300K. The reported values of τ for GaN, AlN and InN are 32.5ps, 16.5ps and 47.2ps respectively. Hence it can be said that ultrasonic attenuation due to phonon-phonon interaction in w-BN will exist near to the ultrasonic attenuations of InN.

Conclusion

On the basis of above discussion, we conclude that our potential model approach theory for evaluation of second order elastic constants is justified for w-BN. The parameters density, elastic constant, ultrasonic velocity, Debye temperature, thermal relaxation time and thermal conductivity of w-BN is found to decrease with temperature while specific heat, thermal energy density is received to increase with temperature. The present temperature dependent properties with known properties of w-BN will open a new dimension for further investigation and application of this material.

Acknowledgements

The authors are highly thankful to Prof. R. R. Yadav, Vice Chancellor, VBS University Jaunpur, U. P. India for his valuable discussion during the course of work. The authors also express their thanks to Dr. S.S.S. Kushwaha, Principal, P.P.N. College, Kanpur for providing necessary facilities and Dr. Shripal, Dr. Renuka Arora, Dr. Satish Chandra, Physics Department, P.P.N. College, Kanpur for their support and encouragement.

References

1 **Levinshtein M. E., Rumyantsev S. L.** and **Shur M. S.**, Boron nitride in properties of advanced semiconductor material: GaN, AlN, InN, BN, SiC, SiGe, 10th ed. *Wiely Interscience Publication, John Wiely and Sons Inc. New York,* (2001) 67-89.

2 **Berger L. I.**, Semiconductor Material,*CRC Press Inc. New York,* (1997) 112.

3 **Meneghetti P., Hans P. J.** and **Shaffer G. W.**, Enhanced boron nitride composition and polymer-based compositions made therewith, *U.S. Patent* (2008) US7445797.

4 **Zhou H. Q., Zhu J. X., Liu Z., Yan Z.** and **Fan X. J. *et al.***, High thermal conductivity of suspended few layer hexagonal boron nitride sheets, *Nano Res.*, **7**(8) (2014) 1232-1240.

5 **Zhou W., Qi S., An Q., Zhao H.** and **Liu N.**, Thermal conductivity of boron nitride reinforced polyethylene composites. *Mater Res Bul.*, **42** (2007) 1863-1873.

6 **Sichel E. K., Miller R. E., Abrahams M. S.** and **Buiocchi C. J.**, Heat capacity and thermal conductivity of hexagonal pyrolytic boron nitride, *Phys. Rev. B* **13** (1976) 4607

7 **Balandin A. A., Ghosh S., Bao W. Z., Calizo I., Teweldebrhan D., Miao F.** and **Lau C. N.**, Superiorthermal conductivity of single-layer graphene, *Nano Lett,* **8** (2008) 902-907.

8 **Shahil K.M.F.** and **Balandin A.A.**,Graphene-multilayer graphene nanocomposites as highly efficient thermal interface materials, *Nano Lett,* **12** (2012) 861-867.

9 **Green J. F., Bolland T. K.** and **Bolland J. W.**, Theoretical elastic behavior for hexagonalboron nitride, *J. Chem. Phys.* **64**(2) (1976) 656-662.

10 **Wentzcovitch R. M., Chang K. J.** and **Cohen M. L.**, Electronic and structural properties of BN and BP, *Phys. Rev.,B* **34** (1986) 1071.

11 **Grimsditch M.** and **Zouboulis E.S.**, Elastic constants of boron nitride, *Journal of Applied Physics*, **76** (1994) 832-834.

12 **Shimada K. , Sota T.** and **Suzuku K.**, First-principles study on electronic and elastic properties of BN, AlN, and GaN, *J. Appl. Phys.*, **84**(9) (1998) 4951-4958.

13 **Solozhenko V. L., Hausermann D., Mezouar M.** and **Kunz M.**, Equation of state of wurtzitic boron nitride to 66 GP,. *Appl. Phys. Lett.*, **72**(14) (1998) 1691-1693.

14 **Kanoun M. B., Merad A. E., Merad G., Cibert J.** and **H Aourag H.**, Prediction study of elastic properties under pressure effect for zinc blende BN, AlN, GaN and InN, *Solid-State Electronics*, **48**(9) (2004) 1601-1606.

15 **Martin R. M.**, Relation between elastic tensors of wurtzite and zinc-blende structure materials, *Phys. Rev. B,* **6**(12) (1972) 4546.

16 **Kittel C.**, Introduction to Solid State Physics, *7th edition John Wiley & Sons, Inc. Singapore, New York*, **17** (2003) 25, 51.

17 **Yadav A. K., Yadav R. R., Pandey D. K.** and **Singh D.**, Ultrasonic study of fission products precipitated in the nuclear fuel, *Mat. Lett.*, **62** (2008) 3258-3261.

18 **Pandey D. K.** and **Pandey S.**, Ultrasonic : a technique of material characterization: in Acoustic Waves, *edited by: Don W. Dissanayake, Scio Publisher, Sciyo, Croatia,* (2010) 397-430.

19 **Pillai S.O.**, Solid State Physics : Crystal Physics , *7th Ed. New Age International Publisher,* (2005) Chap. 4 , pp. 100- 111.

20 **Kittel C.**, Introduction to Solid State Physics, *7th edition John Wiley & Sons, Inc. Singapore, New York*, (2003) 24.

21 **Gray D.E.,** *AIP Handbook IIIrd edition. McGraw Hill Co. Inc. New York*, (1956) pp.4-44, 4-57.

22 **Morelli D. T.** and **Slack G. A.**, High lattice thermal conductivity solids in high thermal conductivity of materials, *Ed. Shinde SL, Goela J. XVIII Ed. Springer Publisher,* (2006) chap 2, pp 37-68.

23 **Shimada K., Sota T.** and **Suzuku K.**, First-principles study on electronic and elastic properties of BN, AlN, and GaN, *J. Appl. Phy.*, **84**(9) (1998) 4951-4958.

24 **Pandey D. K., Singh D.** and **Yadav R. R.**, Ultrasonic wave propagation in IIIrd group nitrides, *Appl. Acoust.*, (2007) 766-777.

25 **Bai-Ru U., Zhao-Yi Z., Hua-Zhong G.** and **Xiang-Rong C.**, Structural and thermodynamic properties of wurtzitic boron nitride from first-principle calculations, *Commun. Theor. Phys.*, **48**(2007) 4925-4929.

J. Pure Appl. Ultrason. 39 (2017) pp. 110-115

Temperature and concentration dependent acoustical analysis of $MgFe_2O_4$ nanoparticles-ethylene glycol liquid suspensions

Alok Kumar Verma[1,*], Aashit Kumar Jaiswal[1] and Raja Ram Yadav[1,2]

[1]Department of Physics, University of Allahabad, Allahabad-211002, India
[2]Veer Bahadur Singh Purvanchal University, Jaunpur-222003, India
*E-mail: alok9369@gmail.com

In present work, $MgFe_2O_4$-ethylene glycol nanofluids of various concentrations have been synthesized using ultrasonication method. The powdered $MgFe_2O_4$ nanoparticles are characterized by X-ray diffraction (XRD) and transmission electron microscopy (TEM). Particle size distribution of the nanoparticles in the base fluid has also been studied with the help of acoustical particle sizer (APS-100). Temperature dependent ultrasonic velocity, adiabatic compressibility and acoustic impedance at different concentration (0.1, 0.2, 0.5, 1.0 and 2.0 vol%) of $MgFe_2O_4$ have been investigated using ultrasonic interferometer. This paper is interested in systematic experimental study on the response of $MgFe_2O_4$-ethylene glycol nanofluids to the ultrasonic wave propagation. The main focus of the study is to understand the particle-fluid interaction and particle-particle interaction as function of concentration and temperature. The obtained results are discussed in correlation with the suitability of the present nanofluids for industrial application.

Keywords: Acoustical particle sizer, nanofluids, $MgFe_2O_4$, ultrasonic velocity.

Introduction

Ferrite nanoparticles have received great attention due to their potential applications in modern technology such as high density magnetic recording, magneto hydrodynamics, optical filters, solar cell, catalysis, and sensors[1-4]. In the upcoming years, ferrites will gain more attention because of its biocompatibility and applications in targeted drug delivery and magnetic hyperthermia[5-6]. Among ferrites, magnesium ferrite ($MgFe_2O_4$), a soft magnetic n-type semiconductor material, has attracted widely in many applications due to its porous and oxygen deficient structure. $MgFe_2O_4$ have a cubic structure of normal spinal type[7-9]. The magnetic, electric and catalytic properties of $MgFe_2O_4$ have been extensively investigated by researchers but studies on acoustical properties which give various physical and chemical characteristics of the system are rarely found[10]. Since the material with same constitution can show different properties with different structure, microstructural property relationship is significantly important[11]. Ultrasonic velocity in combination with attenuation is required for the non-destructive ultrasonic technique of material characterization which can also provide crystallographic texture and improve the scrutinizing ability of materials[12-13]. Ultrasonic velocity is directly related to elastic constants which provide valuable information on the stability and stiffness of the materials.

In the present work $MgFe_2O_4$ nanoparticles have been synthesized by a very convenient and less expensive sol-gel method to achieve chemically homogeneous and fine particles. The structural analysis of $MgFe_2O_4$ nanoparticles are characterized by X-ray diffraction (XRD) and transmission electron microscopy (TEM). Particle size distribution of the nanoparticles in the base fluid is also studied using acoustical particle sizer (APS-100) which is based on acoustical spectroscopy. Colloidal suspensions of $MgFe_2O_4$ nanoparticles in ethylene glycol (EG) are used to prepare magnetic nanofluids by ultrasonication method. EG is used due to its lower freezing point and can be applied in industrial fields as heat transfer fluids, lubricant and coupling agents. Temperature dependent ultrasonic velocity, adiabatic compressibility and acoustic impedance at different concentration (0.1, 0.2, 0.5, 1.0 and 2.0 vol%) of

$MgFe_2O_4$ are investigated using ultrasonic interferometer. The concentration and temperature dependent ultrasonic velocity, compressi-bility and acoustical impedance are carried out for ultrasonic characterization. All these parameters can give insight into materials' microstructure and associated mechanical properties. In this work inter particle interaction and intra particle interaction of $MgFe_2O_4$-ethylene glycol nanofluids and its dependency on physical parameter are realized through the variation in acoustical parameter. The obtained results are discussed in correlation with the suitability of the present nanofluids for industrial application.

Experimental

$MgFe_2O_4$ nanoparticles have been synthesized via sol-gel method. The materials taken initially as precursors are magnesium acetate tetrahydrate $[(CH_3COO)_2 Mg.4H_2O]$, iron nitrate nonahydrate $[(FeNO_3).9H_2O]$ and citric acid monohydrate. All reagents purchased from Merck India were of analytical grade and used without further purification. Initially 100 ml solutions of each of magnesium acetate of 0.1 M and iron nitrate of 0.2 M in double distilled water are prepared with 3 hours magnetic stirring. Solution of the acetate is added drop by drop in the nitrate solution with high speed continuous stirring. Further 50 ml aqueous solution of the citric acid is added in the prepared solution and stirring is continued for another 5 h. The powdered form of magnesium ferrite is obtained by ignition method. The crystalline powder of $MgFe_2O_4$ is annealed at 350°C for 3 h to obtain fine powder. The magnetic nanofluids of $MgFe_2O_4$-ethylene glycol is prepared by sonication method using Sonic Vibracell [Model-VC-505]. No surfactant is used in suspensions for the functionalization of nanoparticles for better dispersability. We have prepared five nanofluids at concentration of 0.1, 0.2, 0.5, 1.0 and 2.0 vol% of $MgFe_2O_4$ nanoparticles in ethylene glycol ($C_2H_6O_2$). All the samples are sonicated with ultrasonicator to form uniform magnetic nanofluids.

The powder sample of synthesized $MgFe_2O_4$ are characterized using X-ray diffraction and transmission electron microscopy. The particle size distribution of dispersed $MgFe_2O_4$ in ethylene glycol is measured by acoustical particle sizer (APS-100). Ultrasonic velocity measurements are performed at frequency 4 MHz with the help of ultrasonic interferometer (M-82S) in temperature range of 30°C to 90 °C at concentration of 0.1, 0.2, 0.5, 1.0 and 2.0 vol% of $MgFe_2O_4$ powder in ethylene glycol. The accuracy of ultrasonic interferometer in measuring ultrasonic velocity is at ±0.1% with an error of measurement of ±0.5% in temperature.

Results and Discussion

The X-ray diffraction pattern of synthesized $MgFe_2O_4$ is recorded at room temperature within 20-80º, 2θ range as shown in Fig. 1.

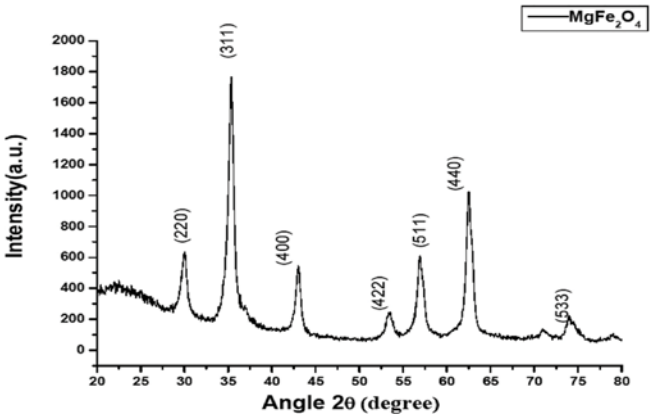

Fig. 1 XRD pattern of $MgFe_2O_4$ nanoparticles

The obtained XRD peaks are identified with the magnesium ferrite peaks (JCPDS card no.36-0398). XRD pattern indicates a face centred cubic structure with lattice constant 8.3873 Å. It can be described as a closely packed cubic arrangement with large unit cell containing eight formula units. The study shows that synthesized magnetic nanoparticles have a single spinal

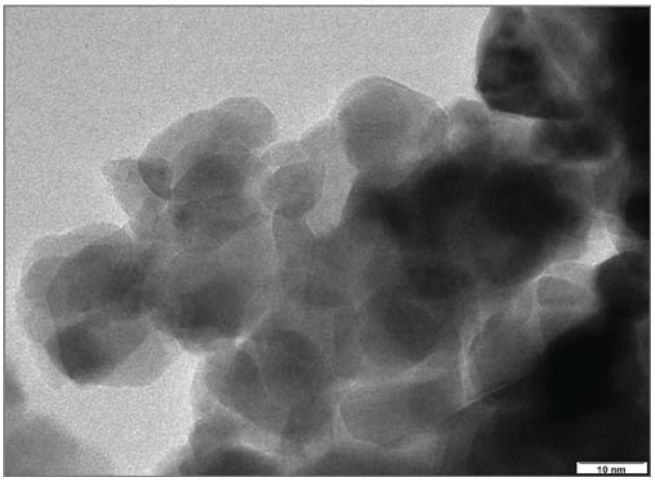

Fig. 2 TEM image of $MgFe_2O_4$ nanoparticles

phase. The crystalline size has been calculated using Scherrer equation: $D = 0.9\ \lambda/\beta \cos\theta$, where β is FWHM (full width at half maxima) in radian, θ is peak position and λ is wavelength of X-ray. The crystalline size at peak positions (220),(311),(400),(422) and (511) planes calculated by Scherrer formula are 14.4, 12.3, 11.9, 7.7 and 11.6 nm respectively, with average crystalline size of about 11.1 nm. Transmission electron micrograph of $MgFe_2O_4$ nanoparticles is shown in Fig. 2.

TEM image indicates that the average size of the $MgFe_2O_4$ lies between 8-20 nm. The average particle size calculated using Scherrer equation is in good agreement with TEM pattern. $MgFe_2O_4$ particles are well dispersed and are in various shapes (irregular polyhedron).

Understanding the changes in the number of particles in EG of a particular size is important to study the agglomeration phenomenon. Particle size distribution of the nanoparticles in ethylene glycol is also determined by APS-100 and is shown in Fig. 3.

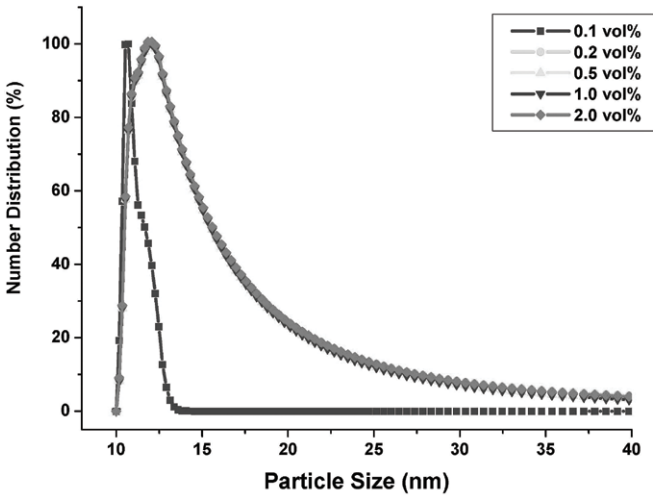

Fig. 3 Particle size distribution of $MgFe_2O_4$ nanoparticles in ethylene glycol

The APS-100 measures the acoustic attenuation (dB/cm) versus frequency of sound in colloidal dispersion with high accuracy. The APS-100 produces particle size distribution data from acoustic attenuation spectroscopy measurement without the need of sample dilution. Figure 3 shows that most of the particles at 0.1 vol% concentration are in the range from 10 to 13 nm. While particles at 0.2 vol% concentration are in the range of 10 to 25 nm which may be because of agglomeration of the particles but when concentration of the nanoparticles increases further, the particle size distribution of the sample remain constant for all concentration of 0.5 vol%, 1.0 vol% and 2.0 vol%. The nanofluids are considered to be stable when the particle size of suspended particles does not change with increase in concentration. Here we can see from the Fig. 3 that particle size distribution is constant for concentration 0.2 to 2.0 vol%. This indicates that the grain growth does not take place on increase of concentration which confirms the making of stable nanofluids. Here in magnetic nanofluids the combined effect of Brownian motion and electric double layer repulsive force dominates over magnetic dipole interaction and van der Waals effect that tries to stick the nanoparticles together[14]. The results of APS-100 are also consistent with XRD and TEM measurements.

Acoustical parameter such as ultrasonic velocity, adiabatic compressibility and acoustic impedance are determined for ferromagnetic nanofluids at different varying physical conditions. A comparative study of these parameters for pure ethylene glycol and magnetic nanofluids for different concentration of $MgFe_2O_4$ nanoparticle in ethylene glycol is done. The variation of ultrasonic velocity for different concentration at room temperature is shown in Fig. 4.

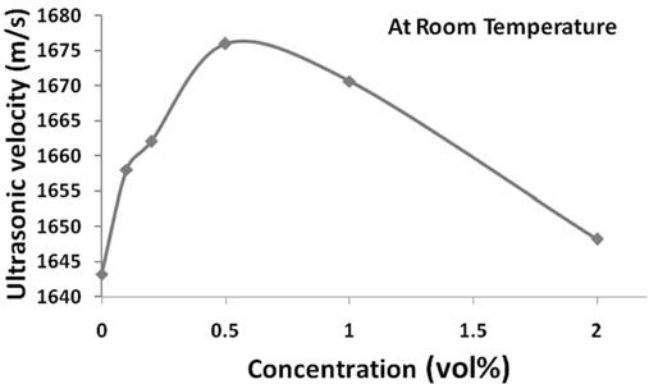

Fig. 4 Ultrasonic velocity versus concentration of $MgFe_2O_4$ nanoparticles in ethylene glycol

It shows that ultrasonic velocity is higher in the nanofluids than pure ethylene glycol. Ultrasonic velocity in nanofluids first increases with concentration up to 0.5 vol% and it decreases afterwards. For very small amount of nanoparticles dispersion in ethylene glycol (<0.5 vol%), the increase of ultrasonic velocity in the particle fluid suspension can be understood with the help of theory of Biwa[15-16]. The equation for ultrasonic

velocity (V) in term of density (ρ) and Lame moduli (λ, μ) is represented as: $V = \sqrt{\frac{B}{\rho}}$, where B = λ+2μ is bulk modulus. An increase in ultrasonic velocity in $MgFe_2O_4$ -EG suspension indicates, there is positive change in density and Lame moduli when the particle is dispersed in the fluid. After dispersion, cohesive interaction forces among molecules/atoms increase largely. Also the change in density is smaller than that of change in bulk modulus. Hence ultrasonic velocity increases with concentration[15]. As the ultrasonic velocity is highly sensitive to local structure, the behaviour of the whole graph may be understood with the help of qualitative measure of particle fluids interaction. One of the reasons for the increase in bulk modulus of nanofluids is that the magnetic nanoparticles have good interfaces with the base matrix which makes strong contacts between magnetic nanoparticle and base matrix. This leads to an increase in bulk modulus of nanofluids in comparison to pure base matrix. Below the critical concentration, the increase in ultrasonic velocity is due to domination of interaction of nanoparticles and fluid particles over intra-molecular interaction between nanoparticles. Further, Brownian motion of the nanoparticles increases which in turn reduces the motion of fluid particles which affect the ultrasonic wave propagation in the nanofluids and hence there is reduction in ultrasonic velocity on increasing concentration.

The change in ultrasonic velocity of $MgFe_2O_4$-ethylene nanofluids temperature for different concentration of nanoparticles is shown in Fig. 5.

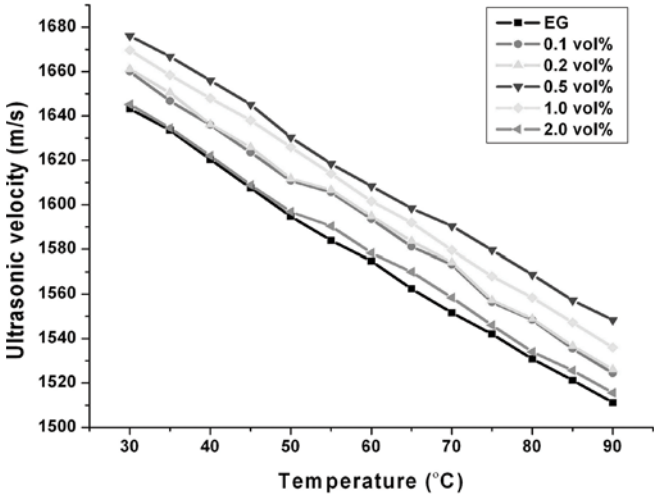

Fig. 5 Ultrasonic velocity versus temperature at different concentrations

Figure 5 indicates that ultrasonic velocity decreases linearly with temperature for all concentration. In water based magnetic nanofluids, ultrasonic velocity generally increases with temperature due to dominating effect of cohesion factor over thermal expansion factor but in ethylene glycol based $MgFe_2O_4$ magnetic nanofluids, the ultrasonic velocity decreases with temperature[1]. As temperature increases the motion of suspended particles in EG is more rapid than that of fluid particles thus the contact time of nanoparticles with their nearest neighbour decreases. Hence, the intermolecular adhesive and cohesive forces decreases with increase in temperature. Finally thermal expansion factor dominates over these two factors which increases adiabatic compressibility leading to decrease in ultrasonic velocity with increase in temperature in ethylene glycol based nanofluids. In general ultrasonic velocity depends upon temperature as: $V = V_o + AT$, where V_o is velocity at initial temperature (0 °C), A is absolute temperature gradient of velocity and T is temperature difference between experimental and initial temperature[15]. It is clear from Fig. 5 that in present magnetic nanofluids the temperature gradient is negative.

Sound wave propagates through adiabatic process rather than thermal process. The adiabatic compressibility (β_{ad}) of the sample fluid is calculated by Newton-Laplace's equation as: $\beta_{ad} = \frac{1}{V^2\rho}$ where ρ is density of nanofluids and V is ultrasonic velocity. This relation is also useful in further determination of elastic properties using the coefficient of adiabatic

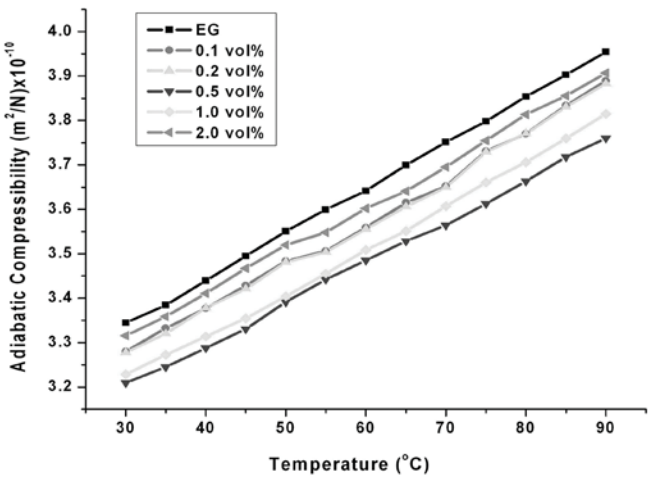

Fig. 6 Adiabatic compressibility versus temperature at different concentrations

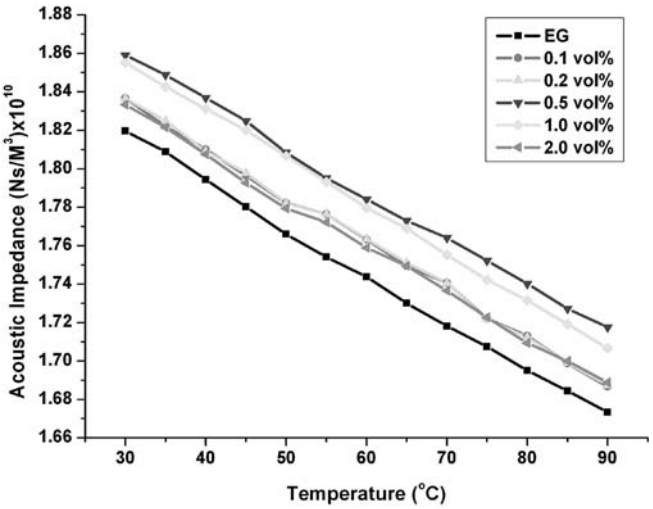

Fig. 7 Acoustic impedance versus temperature at different concentrations

compressibility. Figure 6 shows compressibility of nanofluids with temperature for different concentration. It shows that the adiabatic compressibility of the magnetic nanofluids increases with temperature for all concentrations. As temperature increases, the adiabatic compressibility increases because thermal energy of the system increases with temperature and provides space between molecules. This leads to expansion of volume which in turn increases the adiabatic compressibility. From the figure it is also clear that adiabatic compressibility of the magnetic nanofluids decreases with increase in concentration of suspended nanoparticles up to a critical value of 0.5 vol% which shows significant particle-fluid interaction. It may be due to increased adsorption of nanoparticles on the surface of ethylene glycol molecules because of small size and presence of more surface area of nanoparticles. Hence the formation of closely packed structure of metal ions with molecules of ethylene glycol through hydrogen bonding takes place which causes decrease in adiabatic compressibility. After further increase in concentration, there is less adsorption due to reduced surface area. Hence weak interaction between between molecules of fluids and nanoparticles causes an increase in adiabatic compressibility with concentration[17]. The acoustic impedance is determined by the relation: $Z = \rho v$. Figure 7 shows temperature dependent variation in acoustic impedance at different concentrations.

From the figure it is clear that behaviour of acoustic impedance is almost same as that of ultrasonic behaviour because the change in density of nanofluids is insignificant in compression to change in ultrasonic velocity with concentration of nanoparticles in ethylene glycol. In the present work, inter and intra particle interaction of $MgFe_2O_4$-ethylene glycol nanofluids and its dependency on physical parameter are realized through the variation in acoustical parameter.

Conclusion

In summary, the ultrasonic spectroscopic method for determination of particles size distribution of $MgFe_2O_4$ nanoparticles in ethylene glycol base matrixes as function of concentration is studied. The particle size and its distribution in nanofluids determined with APS-100 are in consistent with TEM. Using experimental data various acoustical parameters are studied in term of concentration and temperature and their dependence on particle-particle interaction and particle-fluid interaction are analysed. Ultrasonic velocity in $MgFe_2O_4$-ethylene glycol nanofluids decreases linearly with increase in temperature for all concentrations. Ultrasonic velocity increases with increase in concentration up to critical concentration of 0.5 vol% due to increase in particle-fluid interaction but beyond this concentration it decreases because of increased particle-particle interaction. Synthesized magnetic nanofluids are highly suitable for industrial applications below the concentration of 0.5 vol% due to significant particle fluids interaction in this range. Present studies are further helpful in determining second order elastic constant of the material.

Acknowledgements

AKV and AKJ acknowledge the financial support provided by the University Grants Commission, India.

References

1 **Rashin M. N.** and **Hemalatha J.**, Magnetic and ultrasonic studies on stable cobalt ferrite magnetic nanofluids, *Ultrasonics* **54** (2014) 834-840.

2 **Singh A., Singh S., Joshi B.D., Shukla A., Yadav B.C.** and T**andon P.**, Synthesis, Characterization, magnetic properties and gas sensing applications of $Zn_xCu_{1-x}Fe_2O_4$ ($0.0 \leq x \leq 0.8$) nanocomposites, *Mat. Sci. Sem. Proc*. **27** (2014) 934-949.

3 **Pankhurst Q.A., Connolly J., Jones S.K.** and **Dobson J.**, Applications of magnetic nanoparticles in biomedicine,

J. Phys. D: Appl. Phys. **36** (2003) R167-R181.

4 **Sharifi I., Shokrollahi H.** and **Amiri S.**, Ferrite-based magnetic nanofluids used in hyperthermia applications, *J. Magn.Magn.Mat.* **324** (2012) 903-915.

5 **Zhang J. , Zhuang J., Gao L., Zhang Y., Gu N., Feng J., Yang D., Zhu J.** and **Yan X.**, Decomposing phenol by the hidden talent of ferromagnetic nanoparticles, *Chemosphere* **73** (2008) 1524-1528.

6 **Veiseh O., Gunn J.W.** and **Zhang M.**, Design and fabrication of magnetic nanoparticles for targeted drug delivery and imaging, *Adv. Drug Del. Rev.* **62** (2010) 284-304.

7 **Lio C., Zou B., Rondinone A.J.** and **Zhang Z.J.**, Chemical control of super-paramagnetic properties of magnesium and cobalt spinal ferrite nanoparticles through atomic level magnetic couplings, *J. Am. Chem. Soc.* **22** (2000) 6263-6267.

8 **Knoch H.** and **Dannheim H.**, Temperature dependence of the cation distribution in magnesium ferrite, *Phys. Stat. Solidi A* **37** (1976) K135-K137.

9 **Grave E. D., Dauwe C., Govaert A.** and **Sitter J. D.**, Cation distribution and magnetic exchange interactions in $MgFe_2O_4$ studied by the mossbauer effect, *Phys. Stat. Solidi B* **73** (1976) 527-532.

10 **Awasthi A., Rastogi A.** and **Shukla J.P.**, Ultrasonic and IR study of molecular association process through hydrogen bonding in ternary liquid mixtures, *Flu. Phase Equil.* **215** (2004) 119-127.

11 **Hussein S.I., Elkady A.S., Rashad M.M., Mostafa A.G.** and **R.M. Megahid**, Structural and magnetic properties of magnesium ferrite nanoparticles prepared via EDTA-based sol-gel reaction, *J. Magn. Magn. Mat.* **379** (2015) 9-15.

12 **Mishra G., Singh D., Yadawa P. K.,Verma S.K.** and **Yadav R.R.**, Study of copper/palladium nanocluster using acoustical particle sizer, *Platinum Metals Rev.* **57** (2013) 186-191.

13 **Verma S.K., Yadav R.R., Yadav A.K.** and **Joshi B.**, Non-destructive evaluations of gallium nitride nanowires, *Mat. Lett.* **64** (2010) 1677-1680.

14 **Hornowski T., Józefczak A., Skumiel A.** and **Łabowski M.**, Effect of poly (ethylene glycol) coating on the acoustic properties of biocompatible magnetic fluid, *Int. J. Thermophys.* **31** (2010) 70-76.

15 **Singh D.K., Pandey D.K.** and **Yadav R.R.**, An ultrasonic characterization of ferrofluid, *Ultrasonics* **49** (2009) 634-637.

16 **Herrmann N., Hemar Y., Lemarechel P.** and **McClements D.J.**, Probing particle-particle interaction in flocculated oil-in-water emulsions using ultrasonic attenuation spectrometry, *Eur. Phys. J. E* **5** (2001) 183-188.

17 **Gupta V., Magotra U., Sandarve, Sharma A.K.** and **Sharma M.**, A study of concentration and temperature dependent effect on speed of sound and acoustical parameters in zinc oxide nanofluids, *Sci.int.*, **4** (2016) 39-50.

J. Pure Appl. Ultrason. 39 (2017) pp. 116-121

Study of molecular interaction in ternary liquid mixture of an aprotic liquid using ultrasonic and viscosity probes

Ashok Kumar Dash[1,*] and Rita Paikaray[2]

[1]Department of Physics, L.N. College. Patkura. Kendrapara-754134, India
[2]Department of Physics, Ravenshaw University, Cuttack-753003, India
*E-mail: ashok.phy@ rediffmail.com

The ultrasonic velocity density and coefficient of viscosity of the ternary mixture of dimethyl acetamide, isobutyl methyl ketone and diethyl ether at frequencies 2MHz, 4MHz, 6MHz and 8MHz have been measured at temperature 308K. Adiabatic compressibility, intermolecular free length, free volume, internal pressure and their respective excess values have been computed for entire range of mole fraction and are interpreted to explain molecular interaction occurring in the liquid mixture. Relaxation time, excess enthalpy and absorption coefficient have been calculated and discussed. The negative excess values of coefficient of viscosity indicate the presence dispersion, induction and dipolar forces in ternary liquid mixture.The negative values of excess adiabatic compressibility, excess free length, excess free volume and excess enthalpy and the positive values of excess internal pressure indicate the presence of specific interactions in the ternary liquid mixture.

Keywords: Ternary mixture, ultrasonic velocity, relaxation time, excess enthalpy, absorption coefficient.

Introduction

The ultrasonic study in organic liquid mixture is interesting to discuss non-linear behaviour with respect to concentration and frequency. The present investigation is related to study of molecular interaction in ternary liquid mixture of dimethyl acetamide which is a dipolar aprotic solvent with high boiling point and good thermal and chemical stability. Dipolar aprotic solvent possesses a large bond dipole moment and a large dielectric constant it does not have O-H and N-H bonds. Ultrasonic studies may throw more light on the molecular interaction to understand the behavior of liquid molecules in ternary mixture of dimethyl acetamide, isobutyl methyl ketone and diethyl ether. The study of DMAC is important because of its utilization in industry and medicine. It is highly soluble in a variety of polar and non-polar liquids and readily suitable to explore solvent-solvent interactions. Isobutyl methyl ketone is a polar solvent used in rare metal extraction, pharmaceuticals, cellulose and resign based coatings. Diethyl ether is a non-polar liquid used as a solvent in the production of cellulose plastics. The physiochemical properties of liquid mixture can be studied by the non-linear variation of ultrasonic parameters with concentration in the liquid mixture[1-8].

Experimental

The ternary liquid mixtures of various concentrations in mole fraction were prepared by taking chemicals of analytical grade which were used as such without further purification. The mole fraction of isobutyl methyl ketone was kept fixed arbitrarily at x_2=0.4. The mole fraction of DMAC was increased from 0 to 0.6 while the mole fraction of diethyl ether was decreased from 0.6 to 0 so as to have the mixture of different compositions. Liquid mixtures of different mole fractions were prepared with a precision of 0.0001 g using an electronic digital balance. Density *(ρ)* of liquid mixture was determined by a specific gravity bottle of 10 ml capacity. Coefficient of viscosity *(η)* of pure liquids and liquid mixture was determined by an Ostwald's viscometer. The ultrasonic velocity *(U)* was measured by a single crystal interferometer with a high degree of accuracy operating at different frequencies (2MHz, 4MHz, 6MHz and 8MHz). An electronically operated constant temperature water bath is used to circulate water through the double walled measuring cell made up of steel containing the

experimental liquid mixture at temperature 308K.

Theory

Using the measured values of density *(ρ)*, coefficient of viscosity *(η)* and ultrasonic velocity *(U)* the acoustical parameters such as adiabatic compressibility (K_s) intermolecular free length (L_f), free volume (V_f) and internal pressure (π_i) have been calculated from the following relations[9].

$$K_s = (U^2\rho)^{-1} \quad (1)$$

$$L_f = k\,(K_S)^{1/2} \quad (2)$$

$$V_f = (MU/k\eta)^{3/2} \quad (3)$$

$$\pi_i = bRT(k\eta/U)^{1/2}(\rho^{2/3}/M^{7/6}) \quad (4)$$

Where *k* is a temperature dependent constant, *M* is the effective molecular weight, *K* is a temperature independent constant which is equal to 4.28×10^9 for all liquids. *R* is universal gas constant, b is the cubic packing factor which is equal to 2 for all liquid mixtures.

The excess values of the above acoustical parameters have been calculated from the following relations.

$$A^E = A_{exp} - (x_1A_1 + x_2A_2 + x_3A_3) \quad (5)$$

Where x_1, x_2 and x_3, are mole fractions of DMAC, isobutyl methyl ketone and diethyl ether respectively and *A* is any acoustical parameter.

Relaxation time *(τ)*, excess enthalpy (H^E) and absorption coefficient (α/f^2), have been calculated from the following relations.

$$\tau = (4/3)\,K_s\eta \quad (6)$$

$$H^E = (X_1\,\pi_{i1}\,V_{m1} + X_2\,\pi_{i2}V_{m2} + X_3\,\pi_{i3}\,V_{m3}) - \pi_iV_m \quad (7)$$

$$\alpha/f^2 = 2\pi^2\tau/U \quad (8)$$

Results and Discussion

The experimental values of density *ρ*, coefficient of viscosity η and ultrasonic velocity at 308K for frequencies 2MHz, 4MHz, 6MHz and 8MHz for pure liquids and ternary liquid mixture were used to calculate the acoustical parameters and the relevant data are presented graphically in Fig. 1-16. Figures 1-3 show that density *ρ* coefficient of viscosity *η* and ultrasonic velocity *U* increase with the increase in mole fraction of DMAC. The increase in density with the increase in mole fraction

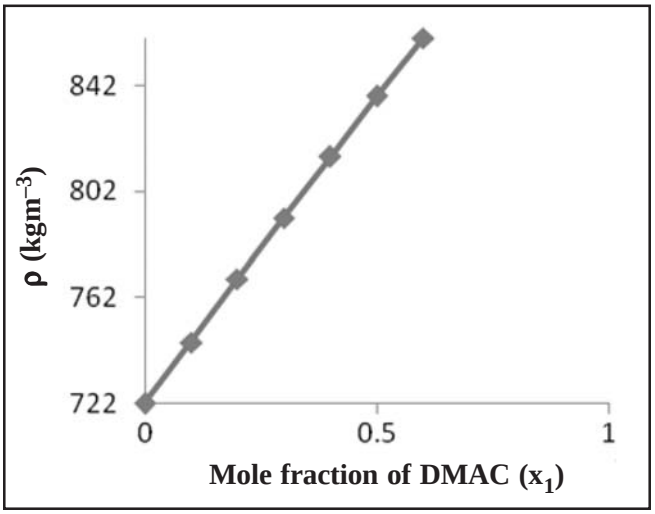

Fig. 1 Variation of ρ Versus x_1

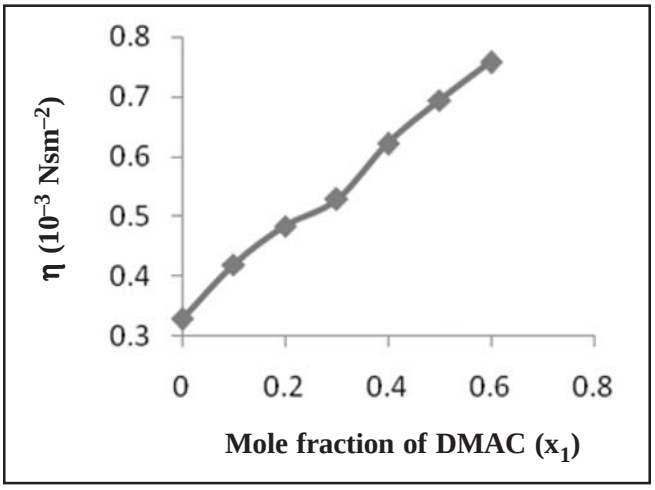

Fig. 2 Variation of η Versus x_1

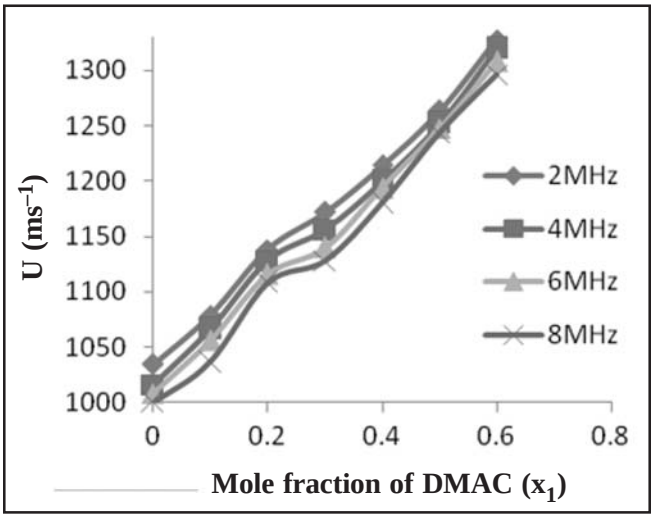

Fig. 3 Variation of U Versus x_1

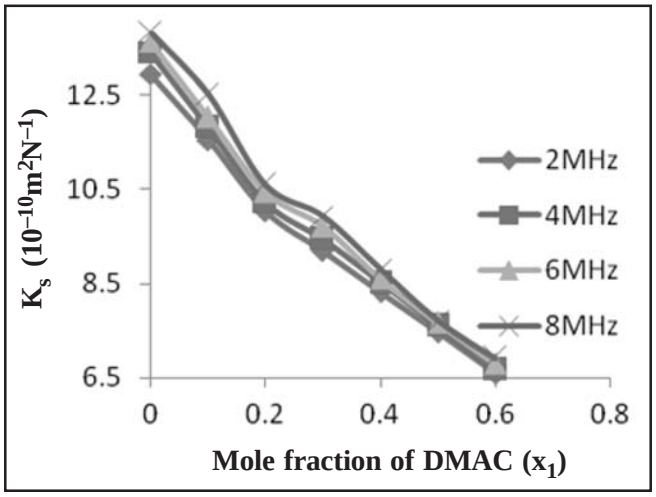

Fig. 4 K_s Versus x_1

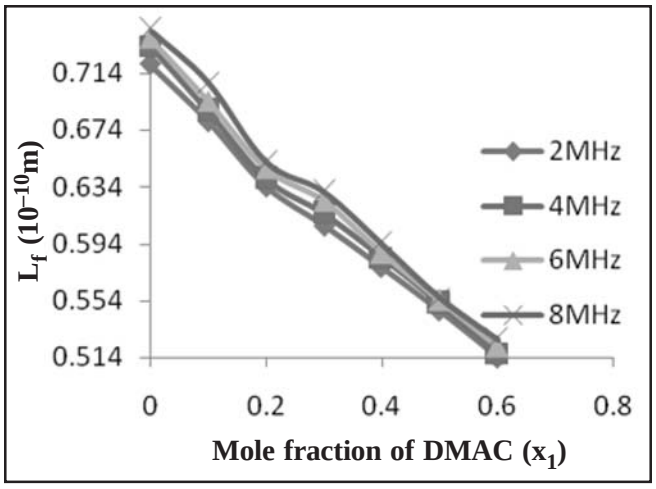

Fig. 5 Variation of L_f Versus x_1

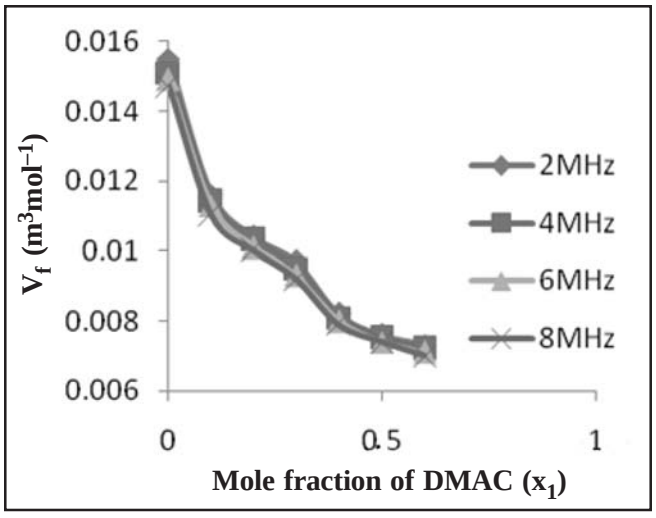

Fig. 6 Variation of V_f Versus x_1

of DMAC indicates the presence of solvent-solvent interactions. The increase in coefficient of viscosity with the increase in mole fraction of DMAC indicates the presence of solute-solvent interactions. The increase in ultrasonic velocity at a particular frequency with the increase in mole fraction of DMAC indicates the increase in intermolecular forces in the ternary mixture. The variations of adiabatic compressibility K_s, intermolecular free length L_f, free volume V_f and internal pressure π_i with the increase in mole fraction of DMAC are shown graphically in Figs. 1-7. The decrease in adiabatic compressibility, intermolecular free length, and free volume while opposite trend in internal pressure with the increase in concentration of DMAC reveal the presence of specific interactions between the components in the liquid mixture.

The ultrasonic velocity decreases at a fixed concentration of DMAC with the rise of frequency from 2MHz, to 8MHz. The decrease in ultrasonic velocity is perhaps due to the decrease in molecular interaction in the ternary liquid mixture. Consequently the values of adiabatic compressibility, intermolecular free length and internal pressure increase and free volume decreases with the increase in frequency for a particular mole fraction of DMAC.

The values of free volume V_f decrease with the increase in mole fraction of DMAC for a particular frequency as shown in Fig. 6. The decrease in free volume with the increase in concentration of DMAC may be due to (i) contraction due to the free volume difference of unlike molecules, (ii) specific interactions between unlike molecules in the liquid mixture.

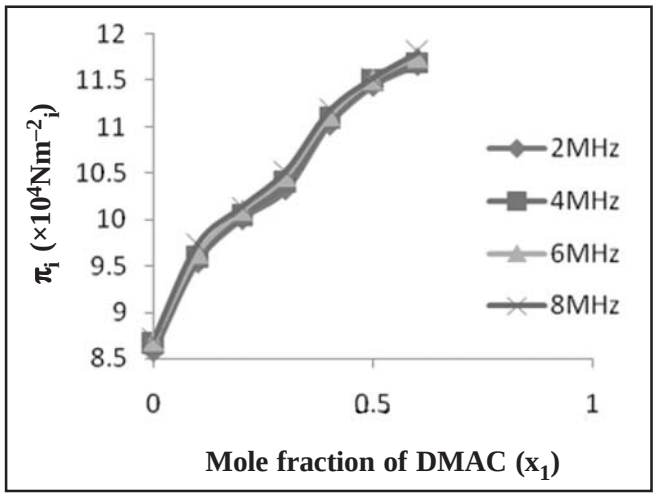

Fig. 7 Variation of π_i Versus x_1

Figure 7 shows that internal pressure π_i increases with the increase in mole fraction of DMAC for a particular frequency. The increase in internal pressure with the increase in concentration of DMAC indicates the increase of cohesive forces in the ternary mixture[10].

The excess values of coefficient of viscosity η^E are negative for the entire range of mole fraction of DMAC as shown in Fig. 8 for all frequencies. The negative excess values of η^E indicate the presence dispersion, induction and dipolar forces in ternary liquid mixture[11].

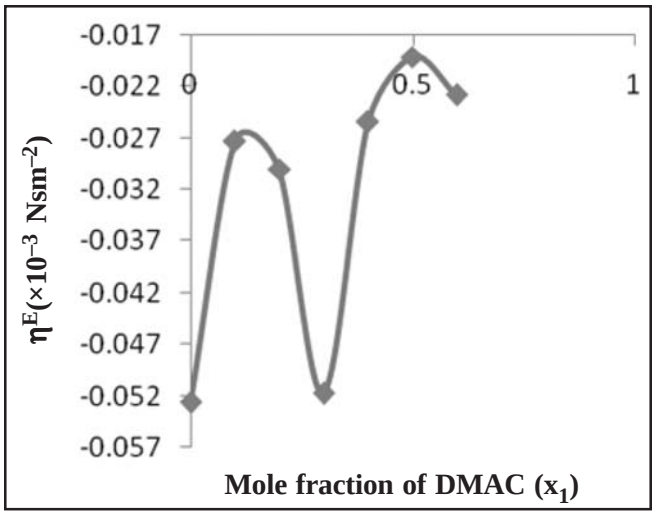

Fig. 8 Variation of η^E Versus x_1

Figure 9 show that the values of excess velocity U^E are positive for the lower concentration and negative for higher concentration of DMAC respectively for all frequencies which indicate the presence of strong interactions at lower concentration and weak interactions at higher concentration of DMAC in the liquid mixture.

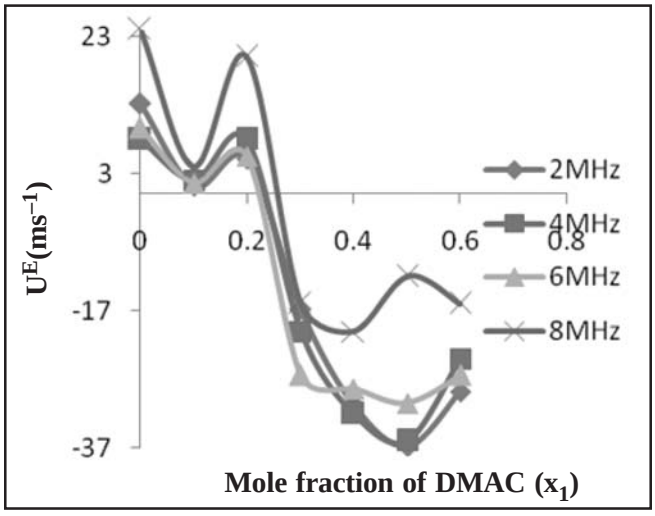

Fig. 9 Variation of U^E Versus x_1

The values of K_s^E are negative as shown in Fig. 10 for the whole range of concentration of DMAC for all frequencies. The negative value of K_s^E predict the existence of strong molecular interactions in the ternary liquid mixture due to charge transfer, dipole-induced dipole and dipole-dipole interactions in the ternary mixture.

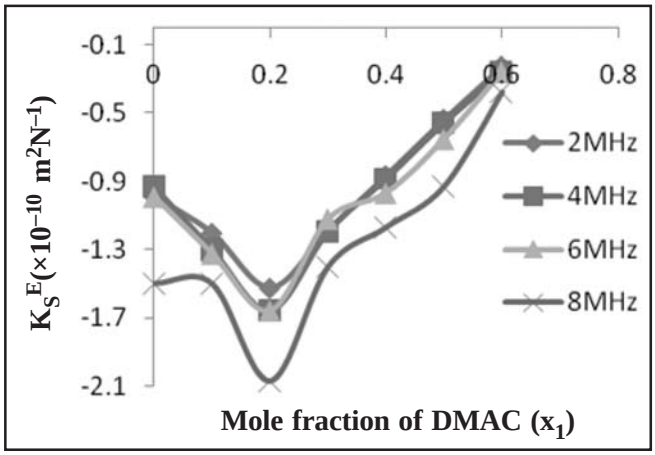

Fig. 10 Variation of K_s^E Versus x_1

It is seen from Fig. 11 that the values of excess free length are negative over the entire range of mole fraction of DMAC for all frequencies. The negative excess values of L_f^E indicate the existence of strong molecular interactions due to charge transfer, dipole-induced dipole and dipole-dipole interactions in the liquid mixture.

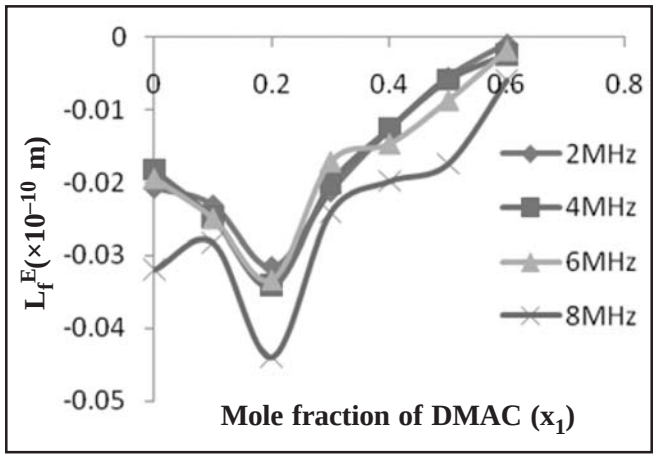

Fig. 11 Variation of L_f^E Versus x_1

Figure 12 shows that the values of excess free volume V_f^E are positive in the absence of DMAC and negative

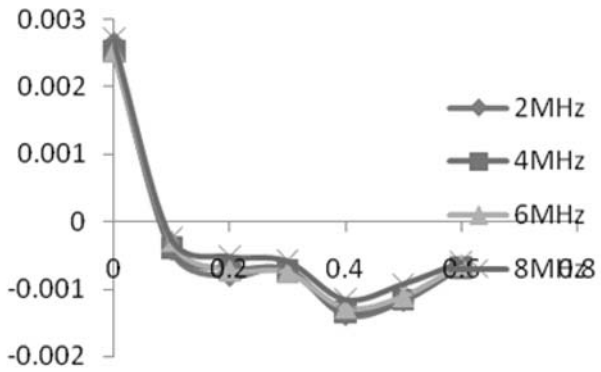

Fig. 12 Variation of V_f^E Versus X_1

for mole fraction of DMAC between 0.1 to 0.6. The values of excess free volume are influenced by (i) the specific interactions between the component molecules and weak physical forces like dipole-dipole or dipole-induced dipole interactions or van der Waals forces (ii) The dispersive forces, steric hindrance of component molecules, unfavorable geometric fitting and electrostatic repulsion. The former effect leads to contraction of volume and the latter effect leads to expansion of volume. In the present investigation the negative values of V_f^E may be interpreted as the contraction of volume of the liquid mixture. The negative values of V_f^E are favorable for the former effect which accounts for the strong molecular interactions in the ternary liquid mixture[12].

The values of excess internal pressure π_i^E are negative in the absence of DMAC and positive for mole fraction of DMAC between 0.1 to 0.6 in the ternary mixture of DMAC as shown in Fig. 13. The positive values of excess internal pressure π_i^E indicate the presence of strong interactions in the liquid mixture[13].

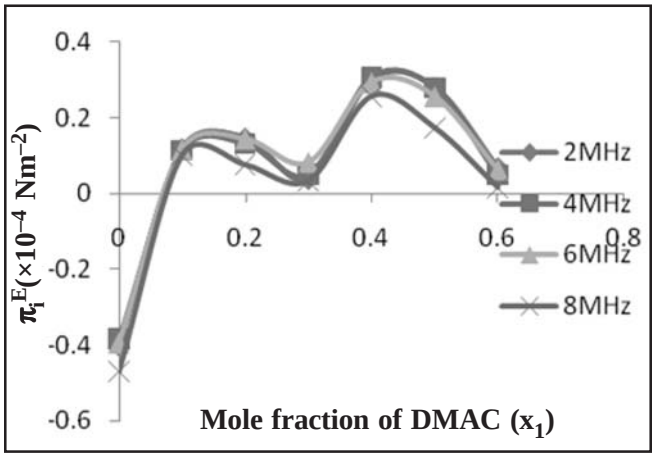

Fig. 13 Variation of π_i^E Versus x_1

It is found that the values of excess velocity, excess adiabatic compressibility, excess free length and excess free volume are changed with the increase in frequency due to the decrease in ultrasonic velocity in the ternary liquid mixture.

It is observed from Fig. 14, that the relaxation time τ varies non-linearly with the increase of mole fraction of DMAC for a fixed frequency. The relaxation time τ increases with the increase in frequency for a fixed mole fraction DMAC. The relaxation time is in the order of 10^{-12}s may be due to the structural relaxation process showing the presence of molecular interactions and in such a case it is suggested that the molecules get rearranged due to co-operative process in the liquid mixture.

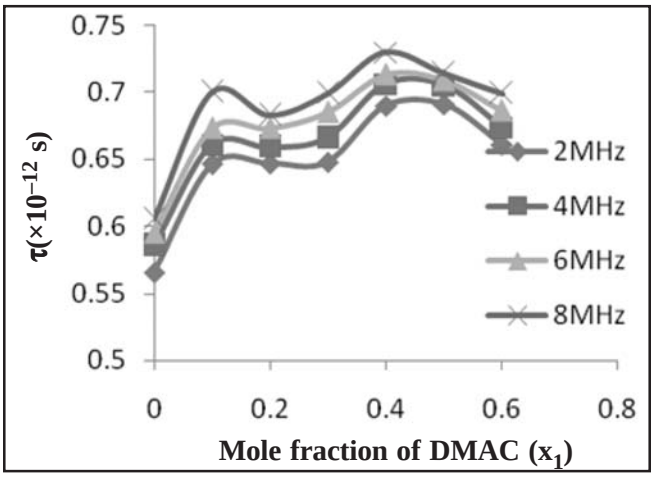

Fig. 14 Variation of τ Versus x_1

Figure 15 shows that the values of excess enthalpy H^E are positive in the absence of DMAC and negative for

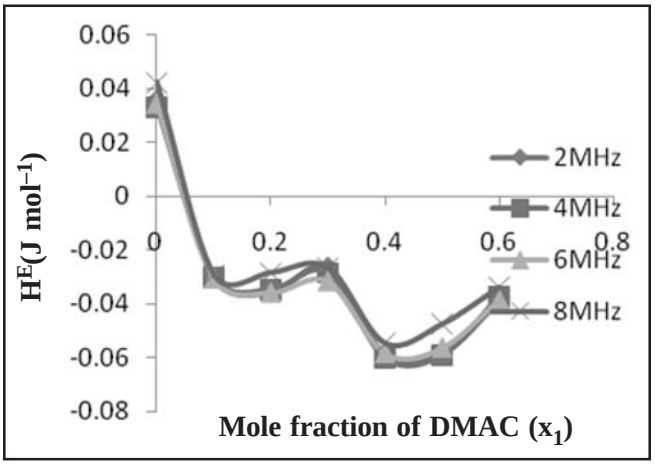

Fig. 15 Variation of H^E Versus x_1

mole fraction of DMAC between 0.1 to 0.6 for all frequencies. The negative values of excess enthalpy H^E indicate the presence of strong interactions in the ternary liquid mixture[14].

The values of absorption coefficient α/f^2 decrease non-linearly with the increase of mole fraction of DMAC as shown in Fig. 16 for a fixed frequency which indicate the increase in molecular interaction[15]. The increase in absorption coefficient with the increase in frequency for a fixed concentration of DMAC indicates the reduction in molecular interaction in the liquid mixture.

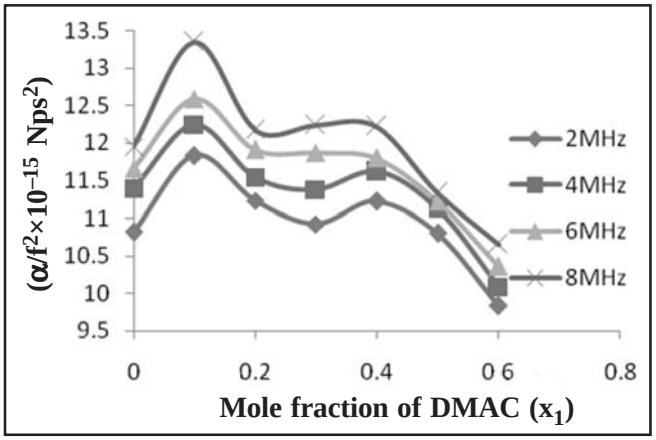

Fig. 16 Variation of α/f^2 Versus x_1

Conclusion

There exists charge transfer, dipole-dipole and dipole-induced dipole interactions and van der Waals forces in the ternary liquid mixture of DMAC, isobutyl methyl ketone and diethyl ether. The molecular interaction increases with the increase in concentration of DMAC for a fixed frequency in the ternary mixture. The molecular interaction decreases with the increase in frequency for a fixed concentration of DMAC in the ternary mixture.

References

1 **Dash A. K.** and P**aikaray R.**, Acoustical study on ternary mixture of dimethyl acetamide (DMAC) in diethyl ether and isobutyl methyl ketone at different frequencies, *Phys. Chem. Liq.*, **51** (2013) 749-763.

2 **Dash A. K.** and **Paikaray R.**, Molecular interaction studies in ternary liquid mixture of dimethylacetamide using ultrasonic technique at 308 K, Phys. *Chem. Liq.*, **53** (2015) 230-241.

3 **Dash A. K.** and **Paikaray R.**, Study of molecular interaction in binary liquid mixture of dimethyl acetamide and acetone using ultrasonic probe, *Adv. Appl. Sc. Res.*, **4** (2013) 130-139.

4 **Dash A. K.** and **Paikaray R.**, Ultrasonic study on ternary mixture of dimethyl acetamide (DMAC) in diethyl ether and acetone, *Res. J. of Phys. Sc.*, **1** (2013) 12-20.

5 **Ramteke J. N.**, Ultrsonic study on molecular interaction in binary liquid mixture containing α-picolin in ethanol at 301.15K, *Pelagia Res. Lib.*, **3**(3) (2012) 1832-1835.

6 **Dash A. K.** and **Paikaray R.**, Visco metric, volumetric and acoustic studies in ternary mixture of dimethyl acetamide and diethyl ether in an aprotic solvent, *Int. J. Sc. Res.*, (2015) 5-9.

7 **Ali A.** and **Nain A. K.**, Ultrsonic study of molecular interaction in binary liquid mixtures at 30°C, *Pramana-J. Phys.*, **58**(4) (2002) 696-701.

8 **Dash A. K.** and **Paikaray R.**, Studies on acoustic parameters of ternary mixture of dimethyl acetamide in acetone and isobutyl methyl ketone using ultrasonic and viscosity probes, , *Int. J Chm.. Phy. Sc.*, **3** (2014) 69-79

9 **Kanappan V.** and **Santhi J.**, Ultrasonic study of induced dipole-dipole interactions in binary liquid mixtures J. *Indian J. Pure Appl. Phys.* **43** (2005) 750-754.

10 **Natrajan R.** and **Ramesh P.**, Ultrasonic velocity determination in binary liquid mixtures, *J. Pure Appl. Ind. Phys*, **1** (2011) 252- 258.

11 **Palani R. Saravanan S.** and **Kumar R.**, Ultrasonic studies on some ternary organic liquid mixtures at 303, 308 and 313K, *Rasayan J.. Chem.* **2** (2009) 622-629.

12 **Thirumaran S.** and **Rajeswari M.**, Acoustical studies on binary liquid mixtures of some aromatic hydrocarbons with dimethylsulphooxide (DMSO) at 303.15K, *Sch. Res. Lib.*, **2** (2011) 149-156.

13 **Mirgane S. R.** and **Patil S.S.**, An ultrasonic study of acrylates with dodecane-1-ol at 313.15K, *Der. Chem. Sin.*, **3**(6) (2012) 1490-1499.

14 **Mehra R., Pancholi M.** and **Gaur A.K.**, Ultrasonic and thermodynamic studies in ternary liquid system of toluene+1-dodecanol+cyclohexane at 298,308 and 318K, *Arch. Appl. Sc. Res.*, **5**(1) (2013) 124-133.

15 **Mehra R.** and **Malav B.B.**, Acoustic,volumetric and visco metric studies in aqueous galactose solution in the presence of sodium chloride 298,308 and 318K, *Res. J. Pharm. Bio. Chem. Sc.*, **2**(3) (2011) 709-719.

J. Pure Appl. Ultrason. 39 (2017) pp. 122-126

Study of thermodynamic properties in binary liquid mixtures through ultrasonic measurement

A. Mathana Gopal and J. Poongodi*

Department of Physics, Kamaraj College, Thoothukudi-628003, India
*E-mail: poongodinagaraj@gmail.com

To understand the intermolecular interactions in organic liquids and liquid mixtures, the study of ultrasonic and thermodynamic parameters are of due importance. Ultrasonic velocity, density and viscosity have been measured experimentally in the two binary mixtures of ethanol and isopropyl alcohol with benzene at different temperature over the entire composition range. The thermodynamic and other allied parameters like free length, internal pressure, enthalpy etc., have been computed and the variation of the excess parameters like excess free volume, excess internal pressure, excess enthalpy, *etc*., is analyzed in the light of intermolecular interactions in the mixtures. The variation of these parameters as a function of solvent composition has been discussed from the view point of intermolecular interactions present between the unlike molecules. In both the mixtures intermolecular interactions between the constituent molecules are suggested.

Keywords: Ultrasonic velocity, free volume, internal pressure, molecular interactions.

Introduction

The ultrasonic absorption studies find extensive application, as the ultrasonic velocity in liquids and liquid mixtures is intrinsically related with many parameters characterizing the physico-chemical behavior of the system such as molecular association, equilibrium constant, thermodynamical parameters, *etc*.,[1-5]. The study of liquid mixture is very important to undertake the physicochemical behavior of liquids and their mixtures, it has inspired many workers and extensive investigations have been carried out in both binary and ternary liquid mixtures using various methods. Measurement of ultrasonic velocity and other acoustical properties have been done to study physico-chemical behavior and molecular interactions in a number of binary system[6,7] .

Thermodynamic and transport properties of liquid mixtures have been extensively used to study the departure of real liquid mixture from ideality. Internal pressure a fundamental property of the liquid state has been studied initially by Hildebrand *et al*. and subsequently used to investigate molecular interaction of binary liquid mixtures. Collin used thermodynamic and ultrasound measurements to determine the internal pressure of liquids, while the effect of the change in the composition and temperature on the excess free volume and internal pressure of binary mixtures have been evaluated by several other workers[8]. As a part of research concerning the thermo chemical studies, we present here some useful data on speed of sound and excess values of free volume, internal pressure and enthalpy were also calculated for the mixtures of ethanol and isopropyl alcohol with benzene at 303K, 313K and 323K over the entire concentration range.

Experimental

Chemicals used for our study were of AR grade and are used without further purification. All the binary mixtures were prepared and were kept in special air-tight bottles. The density of pure liquid and mixtures was determined with a specific gravity bottle with 10 ml capacity. The ultrasonic velocities in pure liquid and liquid mixtures were measured using single-crystal variable path ultrasonic interferometer operating at 2 MHz frequency. The temperature stability is maintained by circulating thermostat water around the interferometer cell that contains experimental liquid.

Theory

The experimentally measured ultrasonic velocity (U), density(ρ) and viscosity(η) are used to calculate the derived parameters such as free volume(V_f), internal pressure(π_i), enthalpy(H) and other related parameters and their excess values are calculated using the following expressions:

1. Molar Volume $V_m = M/\rho$ (1)
2. Free Volume $V_f = (M\ U/K\eta)^{3/2}$ (2)
3. Internal pressure $\pi_i = bRT.(V_f V_m^{\ 2})^{-1/3}$ (3)
4. Enthalpy $H = \pi_i\ V_m$ (4)

All the excess parameters are computed employing the general formula,

$$A^{excess} = A^{expt} - A^{ideal}$$

$$A^E = A^{expt} - (A_1\ x_1 + A_2\ x_2) \quad (5)$$

where A is any parameter (V_m, V_f, π_i, H etc.,) and x_1 and x_2 are the mole fractions of the constituent liquids. Other important parameters involved in the above computations have been explained elsewhere[9].

Results and Discussion

Ultrasonic velocities, densities and viscosities have been measured experimentally in the mixtures of ethanol, isopropyl alcohol with benzene at 303K, 313K and 323K over the entire concentration range and are presented in Table 1. In this binary mixture, velocity decreases with mole fraction of isopropyl alcohol. Other thermodynamic parameters such as free volume, internal pressure and enthalpy are calculated from the experimental data using the above formulae and are presented in Table 2. Their excess values are calculated and are also given in Table 2 and are also plotted from the Figs. 1-3.

A perusal of the data given in Table 1-2, explains the trend of change in velocity, density, free volume, internal pressure and enthalpy with the change in the composition for binary mixture as well as with temperature studied here. In this binary mixture, deviation from the linearity is observed at all temperatures which explain the presence of molecular interaction due to adhesive and cohesive forces between unlike molecules.

Table 1 – Values of U, ρ, η and V_m for the binary liquids at 303K, 313K, 323K

X_2	Velocity U (ms^{-1})	Density ρ (kg/m^3)	Viscosity η ($mNsm^{-2}$)	V_m ($m^3\ 10^{-6}$)
		Ethanol + Benzene		
303K				
0.000	1256	0.869	0.588	89.90
0.603	1172	0.815	0.805	72.18
1.000	1116	0.781	0.949	58.99
313K				
0.000	1228	0.858	0.497	91.05
0.602	1168	0.805	0.676	73.08
1.000	1100	0.772	0.794	59.68
323K				
0.000	1184	0.847	0.437	92.23
0.602	1116	0.798	0.577	73.72
1.000	1060	0.763	0.670	60.38
		Isopropyl Alcohol + Benzene		
303K				
0.000	1256	0.869	0.588	89.90
0.602	1148	0.812	1.299	82.86
1.000	1104	0.777	1.770	77.36
313K				
0.000	1228	0.858	0.497	91.05
0.602	1124	0.803	0.999	83.78
1.000	1088	0.767	1.331	78.37
323K				
0.000	1184	0.847	0.437	92.23
0.602	1089	0.793	0.722	84.84
1.000	1056	0.758	0.911	79.30

Table 2 – Values of V_f, π_i, H, V_f^E, π_i^E & H^E for binary liquids at 303K, 313K, 323K.

X_2	Free Volume V_f (m^3)	Internal Pressure π_i (MPa)	Enthalpy H ($kJmol^{-1}$)	Excess Free Volume V_f^E (m^3)	Excess Internal Pressure π_i^E (MPa)	Excess Enthalpy H^E ($kJmol^{-1}$)
			Ethanol + Benzene			
303K						
0.000	0.243	402.34	36.17	-	-	-
0.602	0.800	313.08	22.59	0.32	-79.44	-5.51
1.000	0.639	386.03	22.77	-	-	-
313K						
0.000	0.303	382.886	34.861	-	-	-
0.602	1.035	294.376	21.512	0.42	-77.58	-5.47
1.000	0.816	364.729	21.766	-	-	-
323K						
0.000	0.347	374.424	34.534	-	-	-
0.602	1.226	285.441	21.042	0.49	-73.80	-5.40
1.000	0.998	349.209	21.085	-	-	-
			Isopropyl + Benzene			
303K						
0.000	0.244	402.11	36.15		-	-
0.602	0.463	342.75	28.40	0.14	-50.43	-4.02
1.000	0.368	387.28	29.96	-	-	-
313K						
0.000	0.303	382.70	34.85	-	-	-
0.602	0.665	311.29	26.08	0.21	-49.63	-4.14
1.000	0.552	346.52	27.17	-	-	-
323K						
0.000	0.348	374.29	34.52	-	-	-
0.602	1.032	275.30	23.36	0.33	-53.00	-4.60
1.000	0.932	297.89	23.62	-	-	-

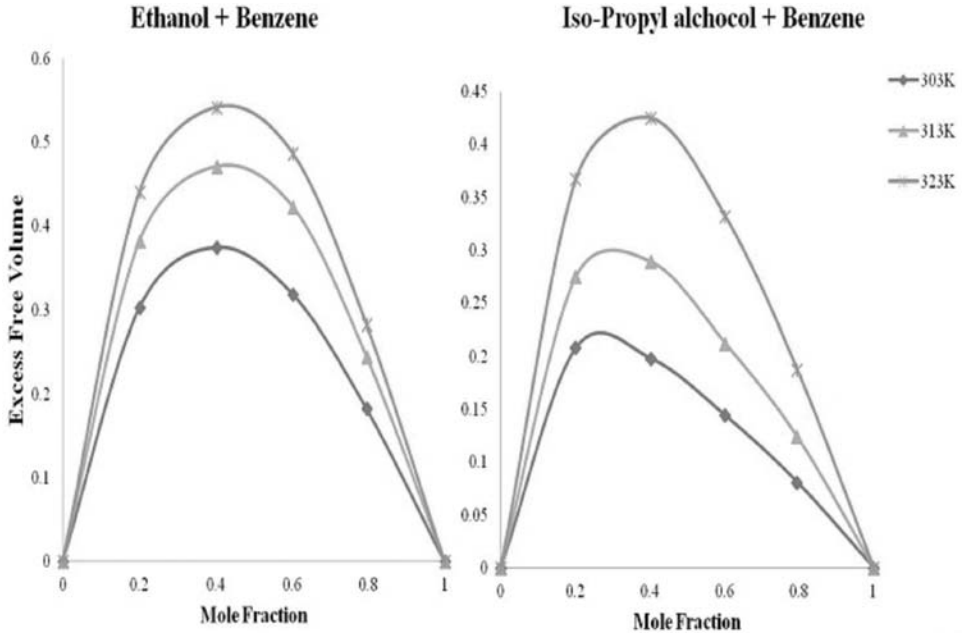

Fig. 1 Variation of excess free volume (V_f^E) with mole fraction (x_2) at different temperature

This in turn gives rise to the positive values of excess free volume and negative values of excess internal pressure. This may be explained qualitatively due to depolymerisation of hydrogen bonded alcohol aggregates, decrease in dipolar association, interstitial accommodation, weak hydrogen bonding interaction

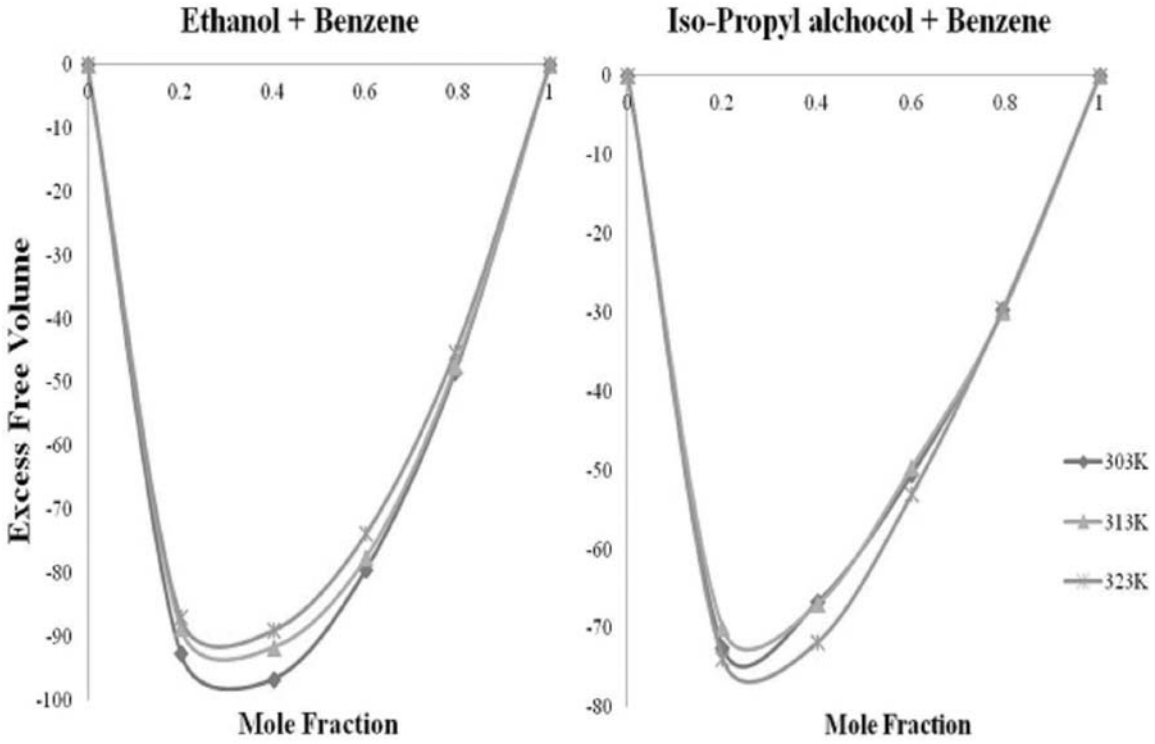

Fig. 2 Variation of excess internal pressure (π_i^E) with mole fraction (x_2) at different temperature

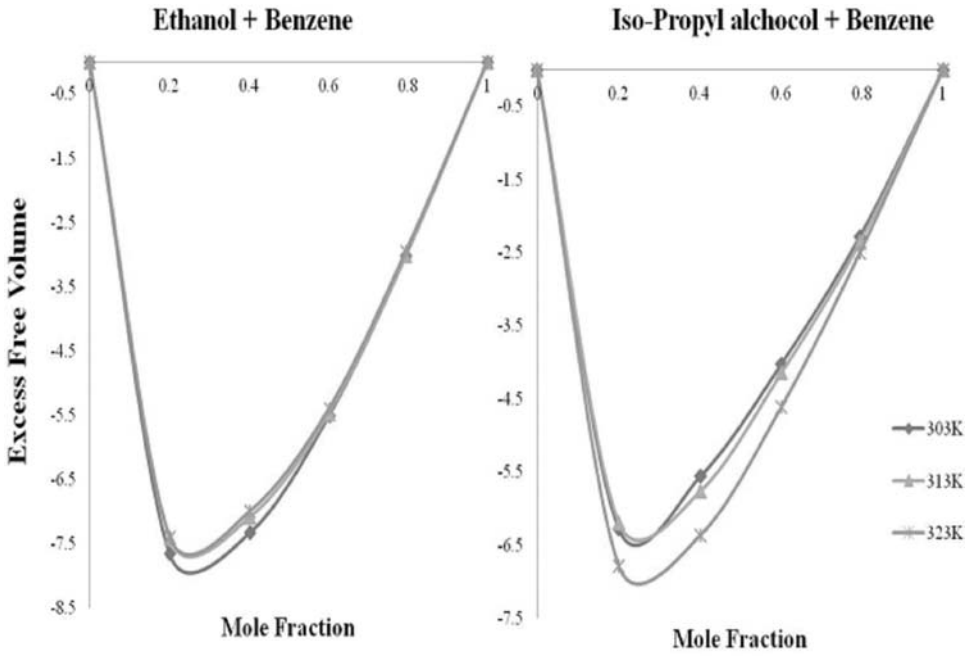

Fig. 3 Variation of excess enthalpy (H^E) with mole fraction (x_2) at different temperature

between unlike molecules and also difference in size and shape. It is also interesting to note that as the temperature increases, V_f^E increases which indicate the disruption of h- bonding. The negative values of π_i^E indicate that only dispersion and dipolar forces are operating. Also increase in temperature cause variation in the experimental values and also in their excess thermodynamic parameters.

Acknowledgements

One of the authors JP, gratefully acknowledged University Grants Commission, for the financial support under Minor Research Project scheme, during the year 2013.

References

1 **Padmasree C., Naidu P.S.** and **Prasad K.R.**, Ultrasonic behaviour of n-butanol in methyl aceto actetate and ethyl chloro propionate, *J. Pure Appl. Ultrason.,* **17** (1995) 28-32.

2 **Natarajan S.** and **Pillai S.O.**, Free Volume of Sodium chloride solutions in water dimethyl formaides: mixtures from ultrasonic velocity, *J. Acoust. Soc. Ind.,* **7** (1979) 75-79.

3 **Chandramouli J., Choudary N.V.** and **Naidu P.R.**, Thermodynamic properties of binary liquid mixtures involving weak interactions Part 1. Excess volume of binary mixtures of 1-cholrobutane with normal alkanols at 303.15K, *Indian J. Pure Appl. Phys.,* **20** (1982) 755-760.

4 **Sivaprasad T.** and **Venkateswarlu**, Ultrasonic studies in binary mixtures of butoxy ethyl at 303.15 K temperatures, *Acoust. Lett.,* **18** (1994) 5-10.

5 **Nagendran S., Poongodi J., Thenappan T.** and **Sabesan R.**, Pseudo-Grüneiser parameters for liquids, *Indian J. Pure Appl. Phys.,* **13** (1991) 3-6.

6 **Nath J.** and **Dixit A.P.**, Ultrasonic velocities and adiabatic compressibilities for binary liquid mixtures of acetone with benzene, toluene, p-xylene and mesitylene at 308K, *J. Chem. Eng. Data,* **29** (1984) 320-324.

7 **Veerbhadriah D., Rajagopal E.** and **Manohara N.**, Excess thermodynamic fluctuation parameters of binary mixtures of benzene, cyclohexane and CCl4 at 198.15K, *J. Pure Appl. Ultrason.,* **19** (1997) 57-63.

8 **Pandey J.D., Shukla A.K., Tripathi N.** and **Dubey G.P.**, Internal pressure, ultrasonic velocity and viscosity of multi-component system, *Pramana.,* **40** (1993) 81-83.

9 **Naidu P.S., Prabhakararao N.** and **Prasad K.R.**, Ultrasonic study and excess thermodynamic parameters of the binary mixtures of 3 methoxy acetophenone and 4 chloroacetophenone containing dimethyl sulphoxide as common component, *J. Pure Appl. Ultrason.,* **24** (2002) 36-39.

J. Pure Appl. Ultrason. 39 (2017) pp. 127-131

Design and analysis of ultrasonic horn for cavitation generation in liquid sodium

B.K Sreedhar[1,*], N. Chakraborty[1], Shaju K. Albert[2] and A.B Pandit[3]

[1]Fast Reactor Technology Group,
Indira Gandhi Centre for Atomic Research, HBNI, Kalpakkam-603102, India
[2]Materials Technology Division, Metallurgy and Materials Group, HBNI, Kalpakkam-603102, India
[3]Department of Chemical Engineering, Institute of Chemical Technology, Mumbai-400019, India
*E-mail: bksd@igcar.gov.in

A vibratory cavitation device is commonly used in the laboratory to study cavitation erosion damage of materials in liquids. These devices are designed and operated in conformance with ASTM-G32 code. The main component of this device is the horn which is used to generate cavitation in the test liquid. The horn operates at ultrasonic frequency and is powered by a piezoelectric crystal driven by an ultrasonic generator. This paper discusses the analysis and design of an ultrasonic horn operating at 20 kHz with peak to peak displacement amplitude of 50 microns at the free end. The free end of the horn is immersed in liquid sodium. The material selection and design of the horn is carried out for a maximum temperature of 550°C. The horn is also provided with features to facilitate sealing of the vessel containing the test liquid (sodium) while ensuring that the necessary amplitude is obtained at the free end without unduly stressing the horn. The analysis is carried out using FEM software and the results are compared with the measured values.

Keywords: Cavitation, vibratory device, ultrasonic horn.

Introduction

A vibratory cavitations device is often used in the laboratory for the study of cavitation because it has several advantages. These are :

(i) It produces high intensity cavitation and therefore is tailor made for the rapid evaluation of materials vis-à-vis their cavitation damage resistance.

(ii) It is simple in construction and operation. Leak tightness, which is paramount while handling hazardous liquids like sodium, can be easily achieved with this device. The vertical construction of the device permits the use of a cover gas above the sodium free surface thus making it possible to achieve leak tightness by the easier method of sealing the cover gas from the atmosphere (rather than the more difficult task of sealing liquid sodium from the atmosphere).

(iii) Testing can be done with a small inventory of liquid

(iv) The method is codified (by ASTM G32-10[1] which standardizes the test procedure and permits comparison of results with published literature.

The vibratory cavitation device generates cavitation in a liquid by the high frequency oscillation of a horn. The horn is a critical component, its functions being (i) to amplify and transmit the ultrasonic vibration at the end of the converter-booster assembly, to which it is mechanically fastened, to the specimen mounted at the bottom of the horn and immersed in the test liquid (ii) to the piezoelectric transducer that generates the ultrasonic vibration away from the test liquid. Figure 1 shows a schematic of the arrangement[2].

The design objective is to achieve maximum amplification of motion in the longitudinal direction without generating undue stress in the horn. Proper selection of material and design of horn geometry is important to ensure that (a) the longitudinal natural frequency of the horn matches the applied frequency (b) the horn is able to withstand the fatigue loading during operation.

We discussed the analysis of horn used in a vibratory cavitation facility used for the study of cavitation damage

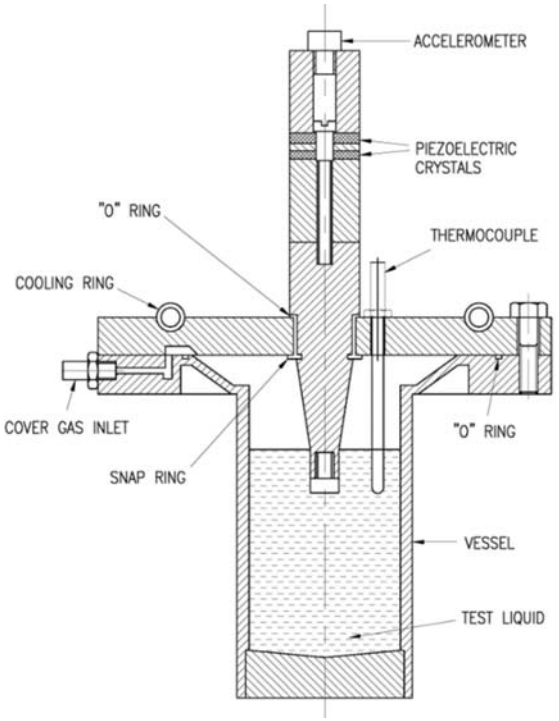

Fig. 1 Vibratory cavitation device

in liquid sodium. FEM analysis is used to determine the longitudinal natural frequency, the axial displacement at the specimen face and the stress distribution along the length of the horn. The vibratory cavitation devices is shown in Fig. 1.

Basic Theory

The oscillation amplitude obtained from the transducer in an ultrasonic system is very small and needs to be amplified for practical application. This amplification is done by using a horn. To maximize the amplification, the horn should be designed to resonate with the system (transducer) frequency. The governing differential equation[3,4] relating the axial displacement at any position along the length of the horn with the axial position is :

$$\frac{d^2u}{dx^2}+\frac{d\ln A(x)}{dx}\frac{du}{dx}+\frac{\omega^2}{c^2}u=0$$

Here u is the amplitude of the vibration in axial direction, $A(x)$ is the cross sectional area of the horn at any axial position x, ω is the angular frequency and c is the sonic velocity, *i.e.* $c=\sqrt{\frac{E}{\rho}}$

where E is the elastic modulus and ρ is the density of horn material. The above can be solved using known boundary conditions $\frac{du}{dx_{x=l}}=\frac{du}{dx_{x=0}}=0$ and $(u)_{x=0} = u_0$. This solution implies the variation of amplitude along the axial direction and determines the resonant length.

Solving this differential equation is limited to regular geometric cross sections such as circular, conical, exponential *etc*. For industrial applications, however, horns may have irregular cross sections to satisfy the appropriate operational requirement and solving the above equations becomes difficult.

For a simple cylindrical horn with one step, the gain in amplitude, k (*i.e.* the ratio of the amplitude of displacement at horn tip (driven end of lower diameter, d) to that at the horn top (driving end of larger diameter, D) is given by $k=\left(\frac{D}{d}\right)^2$ where D is the larger diameter and d is the smaller diameter of the horn[5].

Horn Design

Material selection

The following considerations govern the selection of material of the horn used for cavitation testing :

(i) High fatigue strength: materials with high fatigue strength are preferred as they can be operated at high amplitudes (*i.e.* high stress levels).

(ii) Low acoustic loss.

(iii) Compatibility with the liquid and adequate mechanical strength at the operating temperature

(iv) Resistance to cavitation because a portion of the horn is immersed in the liquid and can experience high impact load from collapsing bubbles

(v) Machinability.

(vi) Availability and cost.

(vii) High yield strength, high impact strength.

Horn geometry

The functions of a horn are *(i)* to amplify and transmit vibrations from the transducer to the specimen immersed in the liquid *(ii)* to keep the transducer away from the liquid (in the case of liquids operating at high temperature, incompatible with horn material *etc.*).

The length of the horn is to be such that a standing displacement wave is formed along its length. Normally the length of the horn is a multiple of half the wavelength[5]. The resonant length of the horn is a function of the operating frequency and the horn material.

The horn diameters are selected such that the diameter of the top of the horn matches with that of the converter-

booster assembly (of the vibratory device) and the diameter at the bottom end matches with that of the specimen (as per ASTM G 32[1]). The horn is mechanically fastened through a threaded joint to the booster of the converter-booster assembly and the diameter of the horn at this location should not be greater than that of the booster to prevent damping of amplitude.

In the cavitation device, for which the horn discussed in this paper is used, the horn is provided with a step/ collar approximately midway along its length to facilitate sealing of the cavitation vessel containing liquid sodium. The step/collar bears against O ring seal on the vessel during operation and provides a leak tight seal. The collar is located at a nodal point so that it does not affect the resonant frequency of the horn/damp the amplitude of vibration.

Dimensional details of horn

The stepped horn used for the experiment is shown in Fig. 2. The material of the horn is high carbon high chromium steel HCHC AISI D2. The maximum dimension of the top of the horn is 24.8 mm. This end is fixed to the booster of the ultrasonic machine by means of internal threads (1/2"×20 UNF). The major portion of the horn is of circular cross section of diameter 15.8 mm. The specimen to be tested is threaded to the bottom end of the horn which is provided with internal threads (M10×1.25). A circular disc of 40 mm diameter is provided at a distance of 189.5 mm from the top of the horn. During operation this disc is pressed against O ring seal on the top of the cavitation vessel and thus seals the sodium in the vessel from the atmosphere. In order to ensure effective sealing and stress free operation of the horn, the disc is located at a nodal point.

The horn was analyzed for stress and deflection along its length during operation at the driving frequency of 20 kHz.

This section discusses the modeling and analysis of the horn.

Material properties of horn

The horn material, HCHC, AISI-D2 tool steel is assumed to be isotropic in nature. Properties of the material[6] are : Density, ρ = 7800 kg/m^3, modulus of elasticity, E = 2×10^{11} N/m^2, endurance strength = 580 MPa at 10^{10} cycles.

FEM Model

Analytical solution for this contour is quiet complicated and may not give the actual solution because of simple assumption. FEM is the most powerful and suitable tool for solving structural engineering problem. Here geometry can be modeled more closely to the actual contour; therefore we have more accurate and precise solution.

The horn is modeled (Fig. 2) in ANSYS using 2 noded 3D beam element (BEAM188) which has six degrees of freedom at each node. These include translations in the x, y, and z directions and rotations about the *x, y* and *z* directions. This element is well-suited for linear, large rotation, and/or large strain nonlinear applications also[7]. The horn along with the specimen of 6 mm thickness is modeled as an integral unit. The accuracy of the model is dependent on the element type, degree of discretization and the fidelity of the boundary conditions. The number of elements was optimized to be 210 based on convergence test. Finite dement model of horn is shown in Fig. 3.

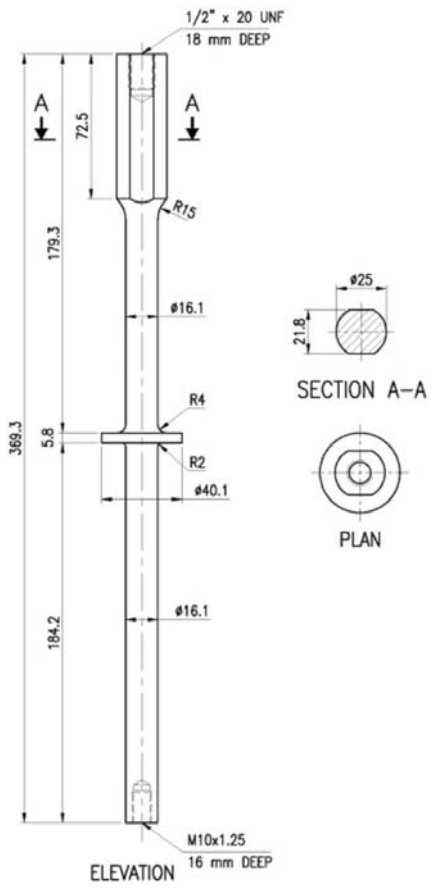

Fig. 2 Ultrasonic horn

Boundary condition

The top of the horn is fixed to the booster of the ultrasonic device and energized at 20 kHz in the longitudinal direction. A parametric study was done for different values of the displacement (zero to peak) at the booster tip (*i.e.* horn top)

Hence the following boundary conditions are used :

At top of horn: u_z = 5.5 μm, 9.5 μm, 10 μm and 11 μm (zero to peak displacement)

$$u_x = u_y = 0$$

The damping coefficient is taken as 2%.

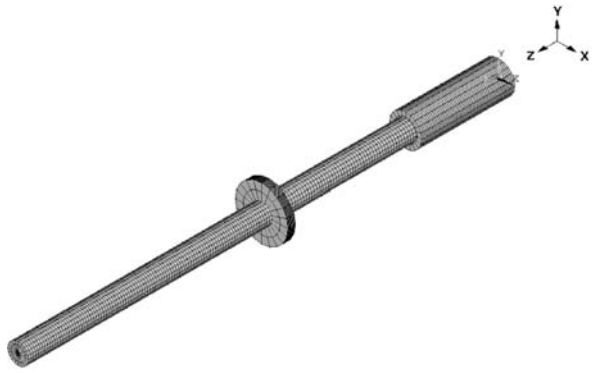

Fig. 3 Finite element model of Horn

Analysis

The first step is to find out the longitudinal natural frequency of the horn that is closest to the driving frequency of 20 kHz. To reduce computational effort mode extraction is carried out in the frequency range 19 - 21 kHz using Block Lanchoz option. The next step is to do harmonic analysis to determine the displacement and stress along the length of the horn with the help of Figs. 4-5.

Results

Natural frequency

The natural frequency of the horn closest to the driving frequency is 20.713 kHz.

Nodal displacement

The displacement and principal stress in longitudinal direction, calculated at 20.5 kHz, are given in Table 1 below. The applied frequency of the ultrasonic generator is 20 ± 0.5 kHz. Hence the frequency closest to the natural frequency of the horn is used for the analysis.

Table 1 – Displacement and stress along the length of horn

Displacement at top of horn (zero to peak), μm	Displacement at bottom of horn (zero to peak), μm	Longitudinal stress, MPa
5.5	13.35	68
9.5	23.07	118
10	24.28	124
11	26.71	136

It is seen that with a driving displacement of 11 μm at the top of the horn, the displacement at the bottom is marginally above 50 μm. The maximum stress in this case, along the centre line of the horn, occurs at the junction of the uniform diameter of 16 mm and the disc of 40 mm diameter. This is because of the large stress concentration at this location.

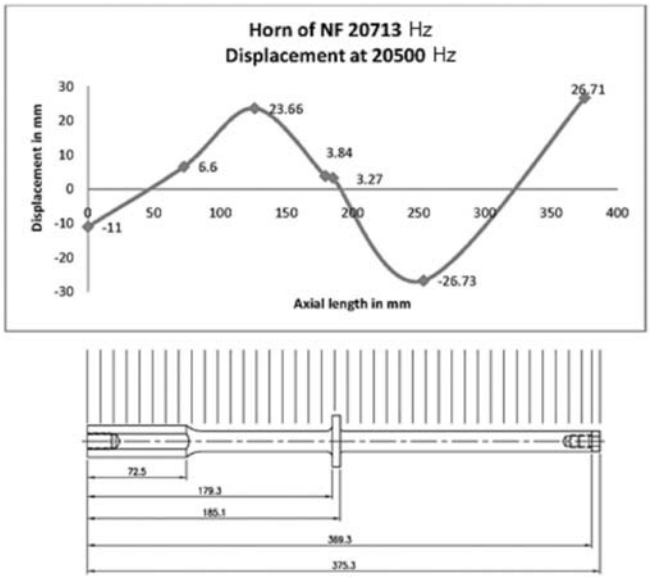

Fig. 4 Displacement along length of the horn

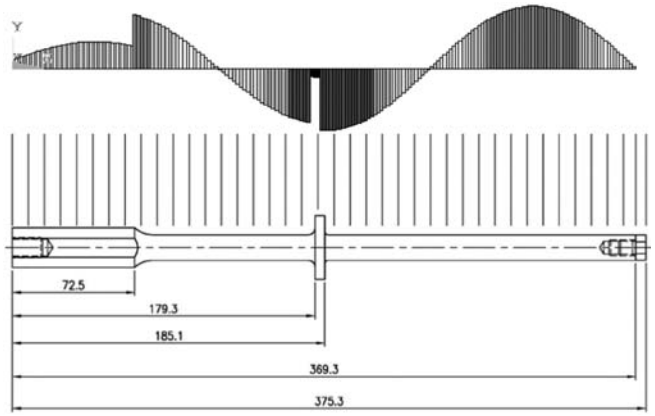

Fig. 5 Stress along length of the horn

It may also be seen from Fig. 4 that the disc of 40 mm diameter is located at a nodal point.

Conclusion

It is important to determine the natural frequency of the horn as well as the amplitude of displacement amplitude along the axis of the horn. This is useful in deciding the support point of the horn which is to be at a nodal point. Another important parameter to be calculated is the axial stress produced along the length of the horn.

In this paper, model analysis was carried out to find out the natural frequency of the horn followed by harmonic analysis at resonance for different input displacements. From the analysis, it is confirmed that the support location of the horn is at a nodal point and the gain in amplitude is proportional to the square of the ratio of larger to smaller diameters. The output amplitude calculated theoretically was confirmed by measurement using a filar microscope.

References

1 **ASTM-G32-10,** Standard test method for cavitation erosion using vibratory apparatus.

2 **Frederick G. Hammitt**, Cavitation and multiphase Flow Phenomena, McGraw Hill, New York (1980) p. 238.

3 **Amin S. G., Ahmed M. H. M.** and **Youssef H. A.**, Computer-aided design of acoustic horns for ultrasonic machining using finite-element analysis. *J. Mat. Proces. Tech.* **55** (1995) 254-260.

4 **Mathias T. L.**, Specimen design for fatigue testing at very high frequencies, *J. Sound Vib.* **247**(4) (2001) 673-681.

5 **Seah K. H. W., Wong Y. S.** and **Lee L. C.**, Design of tool holders for ultrasonic machining using FEM, *J. Mat. Proces. Tech.* **37** (1993) 801-816.

6 **Sohar C. R., Betzwar-kotas A., Gierl C., Weiss B.** and **Danninger H.**, Gigacycle fatigue behavior of chromium alloyed cold worked tool steel. *Int. J. Fatigue*, **30** (2008) 1137-1149.

7 **ANSYS Documentation Release 17.2,** element reference for BEAM188.

J. Pure Appl. Ultrason. 39 (2017) p. 132

Ph.D Thesis Summary

Systematic studies of phase separation in perovskite magnetic materials by measuring ultrasound velocities and attenuation

(Awarded 2017 by Manonmaniam Sundaranar University, Tirunelveli), Tamil Nadu to Dr. P. Thamilmaran, Sri S. Ramasamy Naidu Memorial College, Sattur, Tamil Nadu)

The effect of doping materials on structural/magnetic transition temperatures has been explored in the lanthanum perovskite materials (La-MnO_3/CrO_3) at different concentrations at both the lanthanum and in the Mn/Cr sites. The mixed valent perovskite materials with the general formula $La_{1-x}A_xBO_3$ (A- Barium and Gadolinium and B-Manganese and Chromium) using different values of x using solid state reaction technique.

As for as La site is concerned, $La_{1-x}Ba_xMnO_3$ (LBMO) (x = 0.30, 0.33 and 0.36) and $La_{1-x}Gd_xCrO_3$ (LGCO) (x = 0.0, 0.025 and 0.05) were studied. In the case of B-site, $La_{0.7}Sr_{0.3}Ni_xMn_{1-x}O_3$ (x = 0.01, 0.02 and 0.03) and $La_{0.7}Sr_{0.3}Cu_xMn_{1-x}O_3$ (LSNMO) (x = 0.05, 0.10 and 0.15) were examined. The structural and morphological characteristics of the prepared perovskite samples have been explored employing studies such as X-ray diffraction (XRD), Energy dispersive X-Ray spectroscope (EDX) and Scanning electron microscope (SEM). Further, he carried out the study of the temperature dependence of ultrasonic parameters such as longitudinal velocity, shear velocity, longitudinal attenuation and shear attenuation in order to explicate the phase transition in the prepared perovskite samples.

Both the longitudinal and shear ultrasonic velocities increase with the level of Ba content in the LBMO samples. The elastic constants also show a similar behaviour. However, a reverse trend is revealed in the case of longitudinal and shear attenuation at room temperature.The temperature dependence of ultrasonic measurements was used to explore ferromagnetic (FM) to paramagnetic (PM) phase transition temperature *(T_c)* by the observed anomaly. The value of T_c is 334, 342 and 348 K for the samples with doping level x = 0.30, 0.33 and 0.36 respectively showing an increase in T_c with the increase in Ba content.

In LGCO, the measured values of both longitudinal and shear ultrasonic velocity decreases as the mixing level of Gd increases. The temperature dependence of the ultrasonic parameters in the samples reveals the structural transition from orthorhombic to rhombohedral structure in the samples at the structural transition temperature *(T_S)* 532, 524 and 508 K for the x values of 0.0, 0.025 and 0.05 respectively in the $La_{1-x}Gd_xCrO_3$ perovskite samples. The decrease in T_S with the increase in the level of gadolinium in the sample is due to the decrease in lattice parameters and volume compression of the unit cell which is caused by the shrinkage of the CrO_6 octahedral.

In LSNMO, an anomaly occurred in the measured ultrasonic parameters at the temperatures 373, 358 and 342 K for the x values 0.01, 0.02 and 0.03 in $La_{0.7}Sr_{0.3}Ni_xMn_{1-x}O_3$ samples respectively. Correlation of these temperatures with earlier studies confirmed that they are the Tc values of the samples. The observed decrease in T_c with an increase in Ni content is attributed to the appearance of Ni^{2+} ions in the lattice. This causes the electron-phonon interaction due to JT distortion that leads to the localisation of charge carriers and weakens the DE interaction and enhances the super exchange interaction.

Thus, the researcher explored the effective use of the ultrasonic study, a vital non-destructive evaluation technique for materials characterisation.

LIST OF REVIEWERS

We are highly thankful to the reviewers of the published articles in the Journal of Pure & Applied Ultrasonics, Vol. 39, Nos. (1-4), 2017 for giving constructive commands to improve the quality of the articles.

1. **Dr. S. K. Jain**
   Editor-in-Chief
   Journal of Pure & Applied Ultrasonics
   Formerly Scientist,
   CSIR-NPL, New Delhi
   skjainnpl@yahoo.co.in

2. **Prof. R. R. Yadav**
   Vice-Chancellor,
   VBS Purvanchal University, Jaunpur, U.P.
   rryadav1@rediffmail.com

3. **Dr. Barnana Pal**
   Saha Institute of Nuclear Physics,
   Kolkata-700064, India
   barnana.pal@saha.ac.in

4. **Prof. Siddharth Pandey**
   Department of Chemistry
   Indian Institute of Technology, Delhi
   Hauz Khas, New Delhi-110016
   chempandey@gmail.com

5. **Dr. P. Palanichamy**
   Formerly Senior Scientist,
   Nondestructive Evaluation Division,
   Indira Gandhi Centre for Atomic Research,
   Kalpakkam-603102
   ppc9854@gmail.com

6. **Dr. Anish Kumar**
   Metallurgy and Materials group
   Indira Gandhi Centre for Atomic Research (IGCAR),
   Kalpakkam-603102
   anish@igcar.gov.in

7. **Dr. Sanjay Yadav**
   Senior Principal Scientist
   Ultrasonic Metrology, CSIR-NPL, New Delhi
   syadav@nplindia.org

8. **Prof. Gyan P. Dubey**
   Department of Chemistry
   Kurukshetra University
   Kurukshetra-136119, Haryana, India
   drgyandubey@gmail.com

9. **Dr. Isht Vibhu**
   Physics Department,
   Y. D. P. College, Lakimpur Kheri, U.P, India
   ishtvibhu@gmail.com

10. **Dr. Giridhar Mishra**
    ASET, Bijwasan, New Delhi
    giridharmishra1@gmail.com

11. **Dr. Rita Paikaray**
    Department of Physics
    Ravenshaw University, Cuttack,
    Odisha-753003
    r_paikaray@rediffmail.com

12. **Dr. Sunanda S. Aswale**
    Department of Chemistry
    Lokmanya Tilak College
    Wani, Dist., Yavatmal-445304, Maharastra
    ssaswale@rediffmail.com

13. **Dr. Shashikant R. Aswale**
    Finance Officer
    S.G.B. Amravati University
    Amravati, Maharastra
    sraswale@gmail.com

14. **Dr. Vinod K. Singh**
    Department of Physics
    V.S.S.D. College
    Kanpur-282002, U.P.
    vinodvssd@gmail.com

15. **Dr. Vinay Sanguri**
    Department of Chemistry
    University of Allahabad,
    Allahabad-211002
    drvsanguri@rediffmail.com

16. **Dr. Rakshi Ameta**
    Department of chemistry
    E PAHER University Udaipur, Rajasthan
    rakshit_ameta@yahoo.in

17. **Dr. Gouri Sankar Roy**
    C.E.T. Bhubaneswar, Odisha
    gsroy_2004@yahoo.com

18. **Dr. Saurabh S. Soni**
    Department of Chemistry,
    Sardar Patel University
    Vallabh Vidyanagar
    Dist. Anand, Gujarat.
    soni_b21@yahoo.co.in

19. **Dr. Ganeswar Nath**
    V.S.S. University of Technology
    Burla, Sambhalpur, Odisha
    ganesh_nath99@yahoo.co.in

20. **Dr. Vyoma Bhalla**
    ASET, Bijwasan
    New Delhi-110061
    bhallavyoma@gmail.com

21. Dr. K. Sakthipandi
Sethu Institute of Technology
Kariapatti-626115, Tamil Nadu
sakthipandi@gmail.com

22. Dr. O. P. Chimankar
Department of Physics
RTM Nagpur University,
Nagpur-440033, Maharastra
opchimankar28@gmail.com

23. Dr. K. K. Pandey
Sharda University
Greater Noida, U.P.
kkpandey35@gmail.com

24. Dr. P. K. Yadawa
ASET, Bijwasan, New Delhi
pkyadawa@gmail.com

25. Dr. Arvind Kumar Tiwari
Department of Physics
B.S.N.V.P.G. College, Lucknow-226001, U.P.
tiwariarvind1@rediffmail.com

26. Dr. D. K. Pandey
Department of Physics
P.P.N. College, Kanpur-208001, U.P.
pandeydrdk@rediffmail.com

27. Dr. Ankur Saraswat
School of Environmental Sciences
Jawaharlal Nehru University,
New Delhi
a.sarswat@rediffmail.com

28. Dr. R. K. Shukla
Department of Chemistry,
V.S.S.D. College
Nawabganj, Kanpur-208002, U.P.
rajeevshukla47@rediffmail.com

29. Dr. N. R. Pawar
Department of Physics
ACS College, Maregaon,
Maharastra
pawarsir1@gmail.com

30. Dr. Y. K. Yadav
General Secretary,
Ultrasonics Society of India
CSIR-NPL, New Delhi
ykyadav6969@gmail.com

31. Dr. Devraj Singh
Amity School of Engineering and Technology,
New Delhi-110061
dsingh13@amity.edu

NEW MEMBERS

(List continued after 2016)

LIFE FELLOWS :

LF -106
Dr. Shashikant Rajeshwar Aswale
(Former Principal, Lokmanya Tilak Mahavidyalaya, Vani)
Finance & Accounts Officer,
Sant Gadge Baba Amravati University, Amravati, Maharastra

LF-107
Dr. Rajeev Kumar Shukla
Associate Professor, Department of Chemistry,
Vikramajit Singh Sanatan Dharma College,
Nawabganj, Kanpur-208002, Uttar Pradesh

LIFE MEMBERS :

LM- 326
Dr. Nandkishore N. Padole
Department of Physics
Shri Sai College of Engineering & Technology, Bhadrawati
Distt. Chandrapur-442904, Maharastra

LM - 327
Mr. A. Shanavas
Technical Officer "C"
Naval Physical Occanographic Laboratory
(NPOL) Thrikkakara, Kochi-682021, Kerala

LM -328
Mr. Ajaya Kumar Patnaik
Professor of Chemistry (Retd.)
Quarter No. 509CA
Ravenshshaw University Campus, Cuttack-753003, Odisha

LM -329
Dr. Monalisa Das
Department of Chemistry
Government Women's College, Keonjhar-758001, Odisha

LM -330
Mr. Ashok Kumar Sahoo
Department of Chemistry
Christ College, Cuttack-753008, Odisha

LM -331
Mr. Sunil Kumar Pradhan
Department of Chemistry
Brahman College, Dandisahi,
Kendrapara-754240, Odisha

LM -332
Mr. Rabindra Nath Mishra
Department of Physics,
Ravenshaw University,
Cuttack-753003, Odisha

LM-333
Dr. M. Srilakshmi,
Assisstant Professor,
V R Sidhartha Engineering College,
Kanuru, Panamaluru Mandal,
Vijayawada- 520007
Andhra Pradesh

LM-335
Dr. R Dhayalan
Scinetific Officer, Non-Destructive Evaluation Division
Metallurgy and Materials Group
Indira Gandhi Centre for Atomic Research,
Kalpakkam-603102

LM-336
Dr. Sandeep Kumar Singh
Assistant Professor,
Department of Chemistry,
Vikramajit Singh Sanatan Dharma College,
Nawabganj, Kanpur-208002
Uttar Pradesh

LM-337
Dr. Ashish Kumar Singh
Department of Chemistry,
Vikramajit Singh Sanatan Dharma College,
Nawabganj, Kanpur-208002
Uttar Pradesh

LM-338
Dr. Vikas Singh Gangwar
Department of Chemistry,
Vikramajit Singh Sanatan Dharma College,
Nawabganj, Kanpur-208002
Uttar Pradesh

LM-339
Dr. Gyan Prakash
Department of Chemistry,
Vikramajit Singh Sanatan Dharma College,
Nawabganj, Kanpur-208002
Uttar Pradesh

LM-340
Dr. Deep Gupta
Department of Electronics and Communication Engineering
Visvesvaraya National Institute of Technology (VNIT)
Nagpur-440010, Maharashtra

LM-341
Dr. Naveen Garg
Senior Scientist
Acoustics & Vibrations Metrology
CSIR-National Physical Laboratory
New Delhi-110012

LM-342
Dr. Biswajit Dalai
Department of Physics
Gandhi Institute of Engineering and Technology
Gunupur-765022,
Odisha

LM-343
Dr. Giridhar Mishra
Department of Applied Physics
Amity School of Engineering & Technology,
Bijwasan, New Delhi

LM-344
Dr. M. Arunachalam
Head, Department of Physics
Sri S.R.N.M. College
Sattur-626 203, Virudhunagar District,
Tamil Nadu

LM-345
Dr. P. Suresh,
Department of Mechanical Engineering,
Indian Institute of Technology Madras,
Chennai-600036,
Tamil Nadu

(To be Conted.....)

AUTHOR INDEX
(Volume 39, January – December 2017)

Journal of Pure and Applied Ultrasonics

(INDEXED IN: Indian Citation Index, Google Scholar, i-Scholar, UGC)

INFORMATION FOR AUTHORS

1. Type of Contribution

JOURNAL OF PURE AND APPLIED ULTRASONICS welcomes contributions on all aspects of ultrasonics including ultrasonic studies in medical ultrasonics, NDT, underwater, transducers, materials & devices and any other related topic. Contributions should fall into one of the following classes.

Paper - These should be on original research work contributing to scientific developments. They should be written with a wide readership in mind and should emphasize the significance of the work.

Reviews and Articles - Includes critical reviews and survey articles.

Research and Technical notes - These should be short descriptions of new techniques, applications, instruments and components.

Letters to the editor - Letters will be published on points arising out of published articles and papers and on questions of opinion.

Miscellaneous - Miscellaneous contributions such as studies, interpretive and tutorial articles, conference reports and news items are also accepted. Recommended contribution lengths are: Papers 2000-4000 words. Reviews and Surveys 2000-5000 words; Conference Reports 500-1500 words; News Items, Research and Technical Notes up to 1000 words.

2. Manuscripts

Manuscripts should be typed on one side of the paper in double spacing with 25 mm margin on all sides of A4 size paper. A soft copy of the manuscript in MS WORD for text and MS EXCEL for illustrations and a PDF file thereof may be sent by e-mail or CD/ DVD. Colour images should be formatted as JPEG files. Figures submitted in colour would be published in colour. Colour should be avoided unless it is required in order to convey a message or serve a purpose in the image.

Title - Titles should be short and indicate the nature of the contribution.

Abstract - An abstract of 100-200 words should be provided on the title page of paper and review article. This should indicate the full scope of the contribution and include the principal conclusions.

Mathematics - Mathematical expressions should be arranged to occupy the minimum number of lines consistent with clarity e.g., $(x^2+y^2)/(x-y)^{1/2}$.

Illustration - The line illustrations along with captions should be clearly drawn with black Indian ink. Figures in Excel are preferred.

References - References should be referred to in the text by number only. The reference number should be given as superscript. The corresponding reference shall contain the following information in order; names and initials of author (s)(bold), title of the work, journal or book title (italic), volume number (bold), year of publication in brackets, page number, e.g., **Kumar S. and Furuhashi H.,** Anisotropic divergence controlled ultrasonic transmitter array for three dimensional range imaging, *J. Pure Appl. Ultrason.,* **38** (2016) 49-57.

Units and Abbreviations - Authors should use SI units wherever possible.

The British Institute of Non-Destructive Testing

is organizing **EWSHM Conference 2018**

Abstracts (of no more than 200 words) are invited on all aspects of structural health monitoring. In order to submit online via the link on the BINDT website (http://www.bindt.org/) by 29 December 2017.

WESPAC 2018 New Delhi

"Acoustical Science and Technology for Quality of Life"

November 11-15, 2018
CSIR-National Physical Laboratory

http://www.wespac2018.org.in

wespac2018newdelhi@gmail.com

IMPORTANT DATES

Deadline for Receipt of Abstracts	15 May 2018
Acceptance and Invitation to Submit Manuscripts	1 June 2018
Deadline for Receipt of Manuscripts	1 September 2018
End of Early Bird Registration	1 September 2018
WESPAC 2018 New Delhi	11-15 November 2018